SEMARAK ILMU PUBLISHING

Journal of Advanced Research in Fluid Mechanics and Thermal Sciences

Journal homepage:
https://semarakilmu.com.my/journals/index.php/fluid_mechanics_thermal_sciences/index
ISSN: 2289-7879

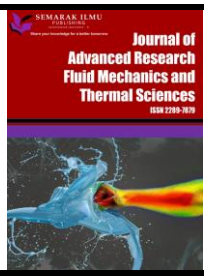

Passive Control of Base Pressure and the Flow Development in a Duct with Sudden Expansion at Sonic Mach Number

Nur Husnina Muhamad Zuraidi[1], Sher Afghan Khan[1,*], Mohd Azan Mohammed Sapardi[1], Saurav Dixit[2,3,4]

[1] Department of Mechanical Engineering, Kulliyyah of Engineering, International Islamic University Malaysia, Malaysia
[2] Lovely Professional University, Phagwara, Punjab, India
[3] Peter the Great St. Petersburg Polytechnic University, Saint Petersburg 195251, Russian Federation, Russia
[4] Division of Research and innovation, Uttaranchal University, Dehradun, India

ARTICLE INFO

Article history:
Received 20 May 2024
Received in revised form 16 October 2024
Accepted 25 October 2024
Available online 10 November 2024

Keywords:
Base pressure; passive control; Computational Fluid Dynamics (CFD)

ABSTRACT

The primary purpose of this research is to investigate the effectiveness of rib as a passive control to control the flow development around the circular duct at different levels of expansion using Computational Fluid Dynamics (CFD). The nozzle pressure ratio (NPR), rib size, and rib orientation were considered in this research. The L/D ratio is from 3 to 5; the simulated NPRs were 1.5, 2, 3, 4, and 5. The rib was designed with a quarter circular shape to see the method's effectiveness. The focus was on the duct's base pressure and wall pressure. The results show that the rib size and orientation strongly influenced the base pressure. The base pressure for the model with rib keeps increasing while the base pressure for the model with plain duct shows opposite results as the NPR increases. The base wall's pressure was not affected by nozzle pressure ratio only. Still, other characteristics, such as rib size and orientation, are significant in manipulating the result. However, the rib does not adversely impact the flow in the duct.

1. Introduction

A nozzle is a device that converts high-pressure fluids into high-speed jets. Nozzles are categorized into three different types. First is the converging nozzle, in which the cross-section of the nozzle decreases from the entrance to the exit. Second, the diverging nozzle has an increasing cross-section from the entrance to the exit. Third, the converging-diverging (C-D) nozzle combines the two nozzles stated earlier. It is also known as the De Laval nozzle. The throat is the most minor cross-section portion of the C-D nozzle. These nozzles are widely used in manufacturing and consumer goods such as gasoline injectors, water jet cutting machines, etc.

The speed of sound in a fluid medium determines the relative speed. The speed of sound can be different according to the fluid medium's pressure and density changes. The Mach number is the speed of an object divided by the speed of sound in a fluid. Subsonic conditions occur for Mach

* *Corresponding author.*
E-mail address: sakhan@iium.edu.my

https://doi.org/10.37934/arfmts.123.2.111139

numbers less than one. When the object's speed approaches the speed of sound, the Mach number is nearly equal to one, M = 1. If the object's speed is greater than the speed of sound, it is called supersonic conditions. Converging nozzles accelerate subsonic fluid flow to sonic velocities, which are less than or equal to the speed of sound (Mach number, M≤1). On the other hand, C-D nozzles are used to accelerate gases to extremely high velocities, such as those exceeding the speed of sound (Mach number, M=1), to extract the maximum thrust required to power an aircraft.

The shear layer divides the base flow into two major zones. The shear layer will generate powerful vortices, increasing the overall drag force. Drag force is the aerodynamic force that resists the motion of an object through the air. The force is formed when a solid body interacts and comes into contact with a fluid. When there is no fluid present, there is no drag. The net drag force is made up of skin friction drag, wave drag, and base drag. Skin friction drag is caused by the physical contact of fluid with the surface of an object, which is called viscosity. Due to solid-fluid interaction, the degree of skin friction drag is affected by the solid and the fluid properties. Rough surfaces have higher skin friction than smooth surfaces. Next, the base drag is caused by the negative pressure originating behind a projectile base. The upstream boundary layer highly impacted the drag. To be precise, the boundary layer is the region of flow where velocity gradients and frictional effects are significant. When the boundary layer separates, it creates a considerable wake that changes the flow downstream of the point of separation. The drag force arises when the boundary layer splits due to flow separation and the presence of the vortex.

Furthermore, shock waves along the surface cause wave drag as an object approaches the speed of sound. The shock waves modify the static pressure and cause total pressure loss. Wave drag is connected to the development of shock waves. The magnitude of the wave drag is proportional to the Mach number of the flow. As a result, shock waves are nothing more than air disruption caused by rapid airflow rates. The base pressure influences the base drag. These two factors are inversely related to one other. When the base pressure rises, the base drag falls, and vice versa. The efficiency of a device improves when the base drag of a bluff body is reduced to the desired level. There is a noticeable difference in the drag form between the subsonic and supersonic flow. In subsonic flow, only skin friction and base drag are present. Skin friction and base drag exist in supersonic flow, and wave drag is introduced.

Based on the scenario of the forced flow of the fluid, two types of fluid flow can be determined. External flow is the flow of an unbounded fluid over a surface, such as a pipe. The second type of flow is internal flow, which can be described as the flow that is bounded by a solid surface, such as flow in a duct or pipe. Nusselt [1] derives the base pressure for high-velocity gas flow by abrupt expansion from three cases of entrance flow regime. When the entrance flow is subsonic, he claims that the base pressure is the same as the entrance pressure. When the entrance flow is supersonic, the base pressure will equal, greater, or less than the entry pressure. When the entrance flow is unity, the expansion waves do not affect any area.

Two types of internal flow in a pipe entirely confined by solid surface conditions of flow present when internal flow past a sudden increase in a compressible fluid was described by Wick [2]. First, the flow is influenced upstream. When the flow at the entry is sonic or supersonic, the flow will be altered. However, when the flow is subsonic, it will be impacted by flow beyond the entry. The pressure at the corner is determined by upstream conditions when the flow in the entrance section is sonic or supersonic.

Moreover, the differences and similarities between these two types of flow were characterized by Wick [2]. There are three significant differences between the internal and external flows. First, only in internal flow can wall shear stresses act on the wake and the reattached boundary layer. Second, the pressure gradients of the paralleled wall sections change as the internal flow of the

sudden expansion changes. Third, the jet boundary will meet at Mach lines, with the expansion waves originating opposite the internal flow corner. However, one similarity between these flows is that both have a wake region. Wick [2] further discusses the impact of the boundary layer on sonic flow. He stated that the boundary layer provided a source of fluid for the corner flow and an insulating layer that affected the pumping effectiveness of the jet. The base corner of the base pressure is the total of two mass supplies; the boundary layer flows around the corner, and the backflow in the boundary layer is along the extended section wall. The pressure in the expansion's corner was connected to the type of boundary layer and the thickness of upstream growth.

Pandey and Rathakrishnan [3] highlighted the expansion flow in the over and under-expanded cases. Both occurrences occur at supersonic speeds. An expansion fan forms at the convergent-divergent nozzle outlet when the flow is under-expanded. Because reattachment occurs early, the length of the reattachment will be reduced. Second, an oblique shock wave will form at the nozzle exit due to over-expanded flow. The reattachment will take longer because the shock prevents the reattachment from occurring. In both circumstances, vortices will appear inside the region between the base and the reattachment point. These vortices will create suction. The suction force's strength is proportional to the length of the reattachment. It can be concluded that the shorter the reattachment length, the higher the strength of the vortices.

Active and passive control are the two approaches to adjusting the base pressure. Base drag can be reduced effectively by controlling base pressure. The eagerness to control the base pressure on abruptly extended flows has inspired many studies, such as Pesce *et al.,* [4], Al-Daraje and Alderoubi [5], and Zhou *et al.,* [6]. Passive control approaches have always captured the interest of researchers since, compared to active control, they offer the desired outcome without the need for any specific apparatus. There is a lot of data obtainable in the literature about abruptly expanded flow issues by Gao and Liu [7], Li *et al.,* [8], Lu *et al.,* [9], and Yan *et al.,* [10] showing the procedures that govern the base flows. Passive controls often involve geometric adjustments to the expanded duct, such as cavities and ribs, and modify the jet control to alter the shear layer's stability characteristics and function as flow control. Passive controls are typically less expensive and easier to build. Cavities such as base and ventilated cavities are among the most often used flow control technologies for flow regulation in abruptly increased flows, and they may boost base pressure based on what the system needs. Pandey and Rathakrishnan [3] studied the flow through an axisymmetric duct with annular cavities spaced at certain distances. They discovered that adding cavity circulation reduces the oscillatory nature of the flow in the enlarged duct, allowing it to increase smoothly from the low pressure to the ambient pressure at which the jet was discharged. Rathakrishnan *et al.,* [11] expanded the analysis to include multiple aspect ratios. They reported that the cavity in the expanded duct had a considerable impact, with the effect being more substantial for longer ducts than shorter ones.

Pandey and Rathakrishnan [12] conducted similar studies for highly subsonic to supersonic flows. They discovered a supplementary circulation to prevent the flow from oscillating due to cavities. This influence was more noticeable in subsonic than supersonic flow regimes. They also found that the enlarged conduit area ratio extensively affects base pressure and flow development. Pathan *et al.,* [13] also produced a similar observation.

Vikramaditya *et al.,* [14] conducted an experimental study to investigate the impact of the base cavity on pressure changes in the base section of a conventional missile system with a high Mach number of 0.7. The primary objective of the investigation was to identify pressure changes and the main factors that drive them. Because the flow is substantially non-uniform, they discovered that the base pressure variation features varied significantly throughout the azimuthal direction due to model asymmetry. They also found that the introduction of the base cavity results in a long-term

improvement in base pressure. Khan *et al.,* [15] explored the advantages of adopting numerous cavities to reduce base drag in compressible subsonic flow. By minimizing base drag, the innumerable holes can regulate the base pressure. They concluded that the longer the duct, the more efficient the control using many cavities. Numerous cavities affect the wall pressure at lower L/D but not higher L/D.

Similarly, the geometric dimensions of the cavity itself determine the base pressure. Khan *et al.,* [15] also further investigated the effectiveness of the dimple in controlling the base pressure at subsonic expanded flow. The base drag will be reduced with an increase in the base pressure. At lower L/D, the wall pressure is affected, but at higher L/D, the wall pressure is not affected. In this case, the base pressure is also influenced by the geometric parameters of the cavities. Furthermore, Asadullah *et al.,* [16] investigate the effect of single and multiple holes on base fluxes. They concluded that many cavities had a substantially more significant impact on base flows than single cavities.

Sethuraman *et al.,* [17] explored suddenly extended duct flows with more significant cross-sectional sizes. They discovered that when NPR increases, the difference in base pressure reduces progressively. The wall pressure of a constant NPR changes continuously over the length of the duct and reaches ambient pressure when the flow passes the duct outlet. Finally, they concluded that the cavity aspect ratio significantly influenced the flow field and base pressure. They also created a low-cost multi-channel data acquisition system (DAQ) and compared it to commercial DAQ. Recent research by Afzal *et al.,* [18,19] on supersonic Mach numbers is based on active control, backed by response surface analysis, k-means clustering, and data backpropagation modeling. For the data analysis, the number of input variables was the same for no control and control.

Ribs, multistep vortex suppression, slotted cavities, dimples, spikes, and other passive approaches are also available. Rathakrishnan [20] investigated the effect of ribs on suddenly expanded axisymmetric flows and discovered that annular ribs significantly reduce the base pressure compared to a passage without a rib. Significantly, the annular ribs with a 3:1 aspect ratio were shown to be more successful at lowering base pressure. Furthermore, they do not generate any significant oscillations in the duct's wall pressure field. In a similar investigation, Vijayaraja [21] used rectangular ribs in the expanded duct and conducted trials under subsonic and sonic conditions. They discovered that adding ribs reduces base pressure to an NPR of three. They concluded that ribs play an essential role in lowering base pressure. Vijayaraja *et al.,* [22] investigated the usefulness of annular ribs in base pressure regulation and flow characteristics for nozzles with abrupt expansion at varied Mach numbers. They discovered that the aspect ratio is vital in determining the base pressure in subsonic and sonic flows.

Three publications were released from prior research for passive regulation of base pressure in the shape of a cavity at supersonic Mach number 1.8 and area ratio 2.56. Ridwan *et al.,* [23] identified a CFD approach to passive base control of pressure utilizing cavities in a sudden expansion duct. They discovered that base pressure is a critical function of the Nozzle Pressure Ratio (NPR), flow inertia, duct length, and ambient pressure. The free stream atmospheric pressure considerably influenced the base pressure for shorter duct lengths. In contrast, the ambient atmospheric pressure impacted the growth of duct flow in smaller-sized ducts. In this situation, the control is effective when under-expanded. For these specific characteristics, Mach number 1.8 and area ratio 2.56, the cavity's base location is 1D from the base wall. Indeed, the ideal geometry is determined by the aspect ratio and other associated characteristics like NPR and Mach number.

Ridwan *et al.,* [24] also studied the effect of cavity position on base pressure at supersonic Mach 1.8. They understood that the cavity in the duct affected the base pressure. Indeed, the higher the base pressure, the larger the distance between the cavity and the base wall. However, the pressure gradient based on the contour data has no negative influence on the base pressure. The latest

research by Zuraidi *et al.,* [25] discovered that the duct cavity influenced the base pressure. The cavity control is effective at correctly expanded and under-expanded nozzle pressure ratios (NPR). As a result, increasing the cavity size does not affect the base pressure.

Furthermore, changing the cavity aspect ratio regarding height does not affect the pressure in the wake. Increasing the cavity width, on the other hand, will affect the pressure in the separated zone. This consequence of recirculation may fall inside the reattachment length and impact the base flow field.

The blowing and suction techniques are part of the active control method. It is also called dynamic flow control, which demands active flow management. Baig *et al.,* [26] explored the airflow from a convergent-divergent nozzle that expanded into a circular duct when the active control approach blew through micro jets. The study concentrated on developing the base pressure and the expanded duct flow. They infer from the supersonic Mach number investigations that microjets can efficiently manage base pressure. In the current study, a specific combination of parameters such as the area ratio, the nozzle pressure ratio, the Mach number, and the duct length-to-diameter ratio resulted in a 45% increase in base pressure. Fharukh and Khan [27] investigated the situation identical to that of Baig *et al.,* [26] but at a more prominent area ratio of 7.56. According to the research, the supersonic Mach number significantly influences the base pressure. The L/D ratios of 4 and 6 have the same effect on base pressure variation as the Nozzle Pressure Ratio. However, the control effect is minimal. The presence of control thus reduces the value of base pressure for Mach 2.7. Asad Ullah *et al.,* [28] also analyzed the impact of active control in the form of micro jets on flow growth in the duct for under-expanded Nozzle Pressure Ratio circumstances precisely. According to the experiment results, the change in the level of under-expansion contributed to the creation of powerful shock waves, leading the wall pressure to be similar to atmospheric pressure or to increase by 20% to 100% from the original wall pressure value. They also concluded that the flow field is interchangeable between control and no-control cases.

Ashfaq *et al.,* [29] looked into the capabilities of micro jets to regulate base pressure in suddenly expanded axisymmetric ducts for area ratios 2.56, 3.24, 4.84, and 6.25 under sonic Mach number conditions. The current study discovered that for lower area ratios, the minimum duct length required for the flow to be linked to the enormous duct wall is L/D = 2, and for higher area ratios, L/D = 3. Microjets' efficiency increases when utilized with a desirable pressure gradient. They can be used as an efficient base pressure controller to adjust the flow field at the duct's base, hence the base drag. Based on the literature, it has been found that numerous experimental works, CFD simulations, and optimization techniques have been utilized to determine the base pressure control of the nozzle sudden expansion duct [30-36]. With this concept, some researchers have performed the CFD simulation to determine pressure around the bluff body and wedge [37,38].

The latest trend of research in this field is using machine learning to predict changes in flow characteristics. Khan *et al.,* [39] used data collection to explore the evolution of compressible flow through a nozzle governed by semi-circular ribs. The goal is to change the base pressure for sonic and supersonic Mach numbers. They used artificial neural networks (ANN), deep ANN (DANN), convolutional NN (CNN), and deep CNN (DCNN) to model the compressible flow data. The data visualization method used in the study reveals that NPR strongly influences the fluid element. The ANN model is the most accurate in predicting base pressure, although the other models produce valuable results. The effectiveness is negligible for over-expanded nozzle flow. When the nozzle flow is at favorable pressure, the flow becomes effective and increases the base pressure.

Similar research was conducted by Khan *et al.,* [40-42] to simulate the base pressure at sonic Mach numbers using rectangular ribs for different area ratios and the control effectiveness of the passive control.

From the above discussion regarding previous studies, the researchers carried out the experiment using ribs as passive control in the shape of annular and rectangular. I want to highlight that for my current work, I am the first person to simulate and observe the flow characteristics using ribs in the shape of a quarter circle. In my study, there are two orientation variants: the curved part of the rib facing the base wall and the flat part facing the base wall.

2. Methodology

In the past, when my existence in this world was still a question mark, the research community made genuine attempts to manage the base pressure and regulate/change the flow field in various ways. Surprisingly, the entire body of work offered by these scientists who devote their lives to science is entirely experimental, utilizing microjets, ribs, or cavities. After sleepless nights of reading and analyzing previous research, no computational study on passive base pressure management has been found to determine the minute details of flow phenomena occurring after the flow expansion utilizing ribs. This article employs ribs as a passive control mechanism, using a computational standard turbulence model and ribs of varying width-to-height ratios. An experimental inquiry is not worth it to achieve the best aspect ratio of the cavity (width to height) and its appropriate location, and comprehending the physics is relatively complex. Because the reattachment site of the shear layer with the pipe, and hence the magnitude of base pressure, is determined by the placement and shape of the ribs.

The study being conducted here focuses on the fluid dynamics aspect of the flow, where fluid flows in the form of air through a converging nozzle are discharged into a duct of a larger cross-sectional area. Using Computational Fluid Dynamics (CFD) for developing numerical models, this paper covers the validation of these models through experimental work by Rathkrishnan [20], who used five ribs at 1D locations at different pressure ratios and Mach numbers ranging from subsonic to sonic. This study uses a single rib with a quarter circular shape as passive control at various aspect ratios, different L/D locations, and different Mach numbers at sonic Mach numbers to further investigate the effectiveness of the passive control methods in breaking the vortex through the use of CFD simulation. In conclusion, the simulations will be run for area ratios of 6.25, utilizing a single rib at different points along the duct at varying degrees of expansion.

Although the computational method has been reliable for decades, it does not accurately describe physical processes; nevertheless, it does offer considerable insight into flow behavior. As a result, choosing the exemplary aspects that closely resemble the flow behavior is necessary. The work identifies the assumptions that jeopardize the precise physical state. The following are the features and presumptions covered in this study. The flow is supposed to be a steady-state two-dimensional, 2D flow due to the flow being symmetric along the flow direction. As for the flow velocity, the turbulent viscous dissipation effects are considerable; hence, the turbulent flow is considered. The fluid is compressible, and its viscosity is a function of temperature. The flows exit from the duct at ambient atmospheric pressure.

Since the flow through the nozzle is considered turbulent, the compressible flow field is represented by the k-ε standard model. As stated by Cengel and Cimbala [43], one of the most popular turbulence models, the k-ε model, offers sufficient accuracy, economy, and durability for various flow conditions. The Ansys Fluent software provides the k-ε turbulence model used in this investigation. The other tested models were the SST, LES, k-w, and one equation models. However, because these models required more computational time and produced comparable results, we decided to stick with the k-ε model. The turbulent kinetic energy, i.e., K-equation, is given by Eq. (1)

$$\frac{\partial(\rho u\mathrm{K})}{\partial z}+\frac{1}{r}\frac{\partial(\rho v\mathrm{K})}{\partial r}=\frac{\partial}{\partial z}\left[\left(\mu+\frac{\mu_t}{\sigma_k}\right)\frac{\partial \mathrm{K}}{\partial z}\right]+\frac{1}{r}\frac{\partial}{\partial r}\left[r\left(\mu+\frac{\mu_t}{\sigma_k}\right)\frac{\partial \mathrm{K}}{\partial r}\right]-\rho\varepsilon+G \quad (1)$$

The kinetic energy of turbulence dissipation, i.e., the ε-equation is given by Eq. (2)

$$\frac{\partial(\rho u\varepsilon)}{\partial z}+\frac{1}{r}\frac{\partial(\rho v\varepsilon)}{\partial r}=\frac{\partial}{\partial z}\left[\left(\mu+\frac{\mu_t}{\sigma_\varepsilon}\right)\frac{\partial \varepsilon}{\partial z}\right]+\frac{1}{r}\frac{\partial}{\partial r}\left[r\left(\mu+\frac{\mu_t}{\sigma_\varepsilon}\right)\frac{\partial \varepsilon}{\partial r}\right]-C_1 f_1\left(\frac{\varepsilon}{\mathrm{K}}\right)G-C_2 f_2\left(\frac{\varepsilon^2}{\mathrm{K}}\right) \quad (2)$$

The geometry model without control, a converging nozzle with a plain duct, as shown in Figure 1, will serve as the benchmark for this work's measurements of the efficiency of passive control and flow development. Passive control is introduced at the duct to manage the flow development further. As seen in Figure 2, the rib is transformed into a quarter circular shape. The ribs' aspect ratio of one is maintained despite variations in their diameters. The ratio of the cavity height to the rib width is known as the aspect ratio. In this work, the cavity locations from the base pressure wall were 1D from the base wall.

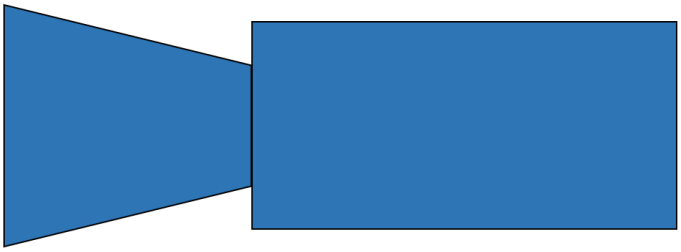

Fig. 1. Geometry model without control

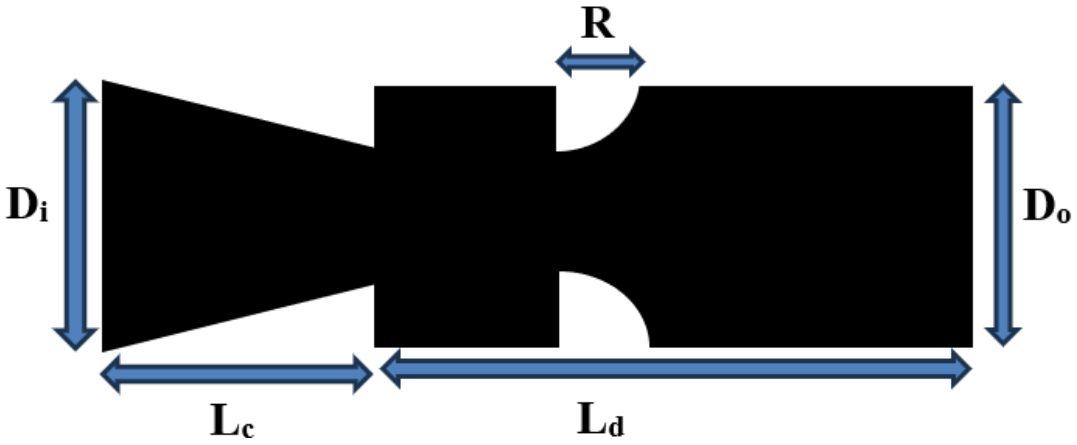

Fig. 2. Converging nozzle model suddenly expanded into a duct with rib

Referring to Rathakrishnan's [20] experimental model, the dimensions for the present work are as follows.

From Table 1, the fixed parameters for this study are nozzle inlet diameter, duct outlet diameter, and nozzle convergent length.

Table 1
The present work dimensions

Nozzle inlet diameter, D_i	30mm
Duct outlet diameter: d_o	15mm
Nozzle convergent length, L_c	20mm
Duct length, L_d	Varies from L/D = 2 to L/D = 6
Rib radius, R	Varies from R = 3mm to 5mm

3. Results and Discussion

The same geometry is used for the mesh independence check. Five different element sizes with different nodes are simulated. Each element size was simulated with different NPR varies from 1.5 to 5.

From the data tabulated in Figure 3, the chosen grid size is the finest size, with several nodes of about 78988 and several elements of 78167. This is because the percentage difference in the base pressure ratio between finer and finest grid sizes is less than 5%. If the element size is reduced and the number of elements increases, iterations will be more than 10k, and the computational time will be higher. So, the most suitable element size is the finest grid size.

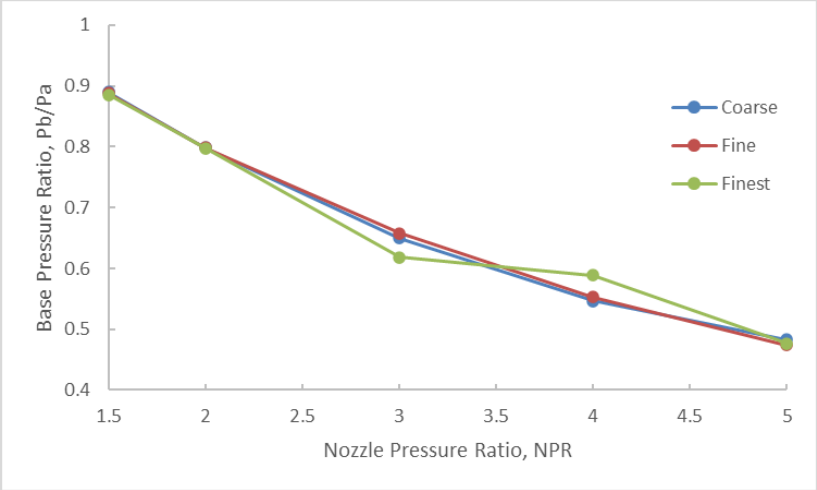

Fig. 3. Five different element sizes have converged values for the mesh independence check

The simulation is validated with the results presented in Figure 2 by Rathakrishnan [20], who performed the experimental work using five ribs placed at central spaces in the duct.

The base pressure ratio data for the current and earlier study by Rathakrishnan [20] are displayed in Figure 4. Dotted lines represented the experimental data, and straight lines represented the Ansys Fluent simulation results. The error percentage was less than 10% compared to the current numerical work and the earlier experimental work. Thus, the current work was completed within the required range. Hence, the validation of the current work was successful based on tabulated data shown in Figure 4.

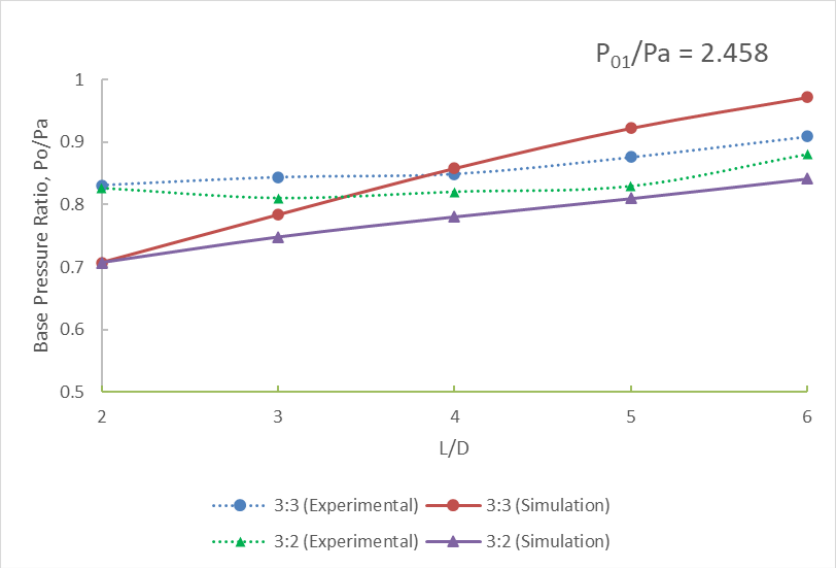

Fig. 4. Validation of previous work by Rathakrishnan [20]

3.1 The Influence of Rib and its Geometry Towards Base Pressure when Length to Diameter Ratio Varies

Figure 5 shows base pressure with L/D ratio at NPR = 1.5 for various rib heights. At this NPR, the nozzle is not choked. In the absence of the rib, the base pressure is nearly constant, which shows that the minimum duct length needed for the flow to remain attached to the duct wall is L = 2D. When ribs of height 3 mm and 4 mm are employed, it reduces the base pressure. Later, with a further increase in the NPR, there is a marginal rise in the base pressure. However, the base pressure pattern for the 5 mm height is different. Until L/D = 3, it has a similar pattern to the other rib heights. There is a decrease in the base pressure for L/Ds in the range 3 to 4. However, for L/Ds in the range 4 to 5, there is a slight increase in base pressure. However, between NPR 5 and 6, there is a substantial increase in base pressure. This may be due to the rise in the height of the ribs to 5 mm, and the nozzle is operated for duct lengths of 5D and 6D. This will result in the formation of secondary vortices at the corner, leading to a rise in the base pressure and ambient pressure, which will influence the base pressure for small duct lengths.

Figure 6 shows base pressure results as a function of L/D ratio when NPR = 2. At this point, the NPR flow has reached critical conditions. In the previous case, when NPR is 1.5, the base pressure values were marginally more than at NPR = 2, as at NPR = 2, the nozzle is ideally expanded, and Mach waves are formed at the nozzle exit, which may be the reason for lower base pressure values. Control decreases the base pressure when the rib height is 5 mm. It may be due to the combined effect of the secondary vortices from the ribs, level of under-expansion, and influence of the backpressure at various L/D ratios. It is well known that at lower L/Ds, ambient pressure will impact the base pressure.

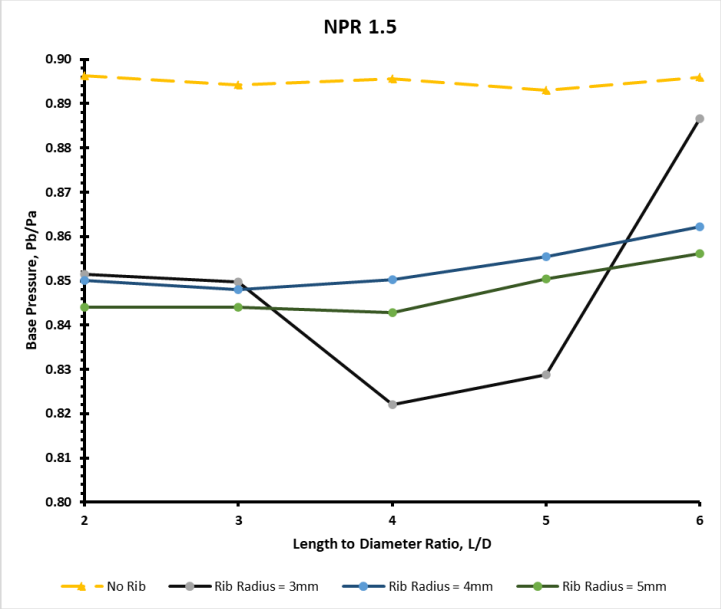

Fig. 5. The base pressure ratio variation with L/D for plain duct and duct with rib at various sizes at NPR 1.5

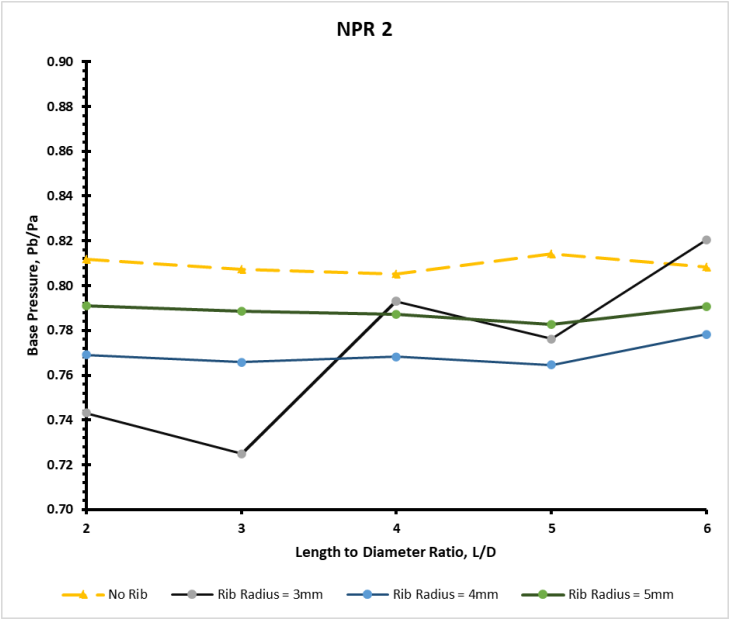

Fig. 6. The base pressure ratio variation with L/D for plain duct and duct with rib at various sizes at NPR 2

Base pressure results as a function of L/D ratio at NPR = 3 is shown in Figure 7. At this NPR, the nozzle is under-expanded, and the level of under-expansion is 1.5 ($P_e/P_a = 1.6$). The figure shows that control has become helpful for 4 mm and 5 mm rib heights. There is an increase in the base pressure, whereas, for a rib height of 3 mm, there is a decrease in the base pressure for all L/Ds. However, a decrease in the base pressure is maximum at L/D = 6, and it may be due to the significant length of the duct that a maximum suction is created. Similar results were obtained by Rathakrishnan [20] for 3 mm rib heights. These results reiterate that whenever the nozzle is flowing under a favorable pressure gradient, the control becomes effective, either passive or active.

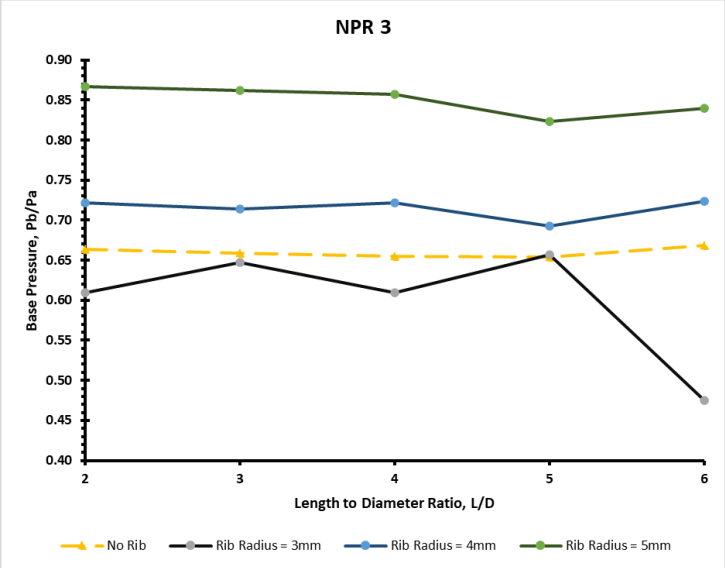

Fig. 7. The base pressure ratio variation with L/D for plain duct and duct with rib at various sizes at NPR 3

When NPR = 4, the base pressure results are displayed in Figure 8. Due to the increase in the NPR, the level of under-expansion has gone up to 2.1 (i.e., $P_e/P_a = 2.1$). The impact of an increase in under-expansion level is demonstrated in this figure. The figure shows that the base pressure increases significantly when the rib height is 5 mm. It is seen that there is a considerable decrease in the base pressure due to the expansion of the nozzle flow at NPR = 4 in the absence of the ribs. At this level of under-expansion, even ribs with 3 mm result in a marginal increase of the base pressure for all the L/Ds except at L/D = 4 and 6. The decrease in the base pressure may be attributed to the duct length, impact of ambient pressure, and interactions if the secondary vortices formed from the sharp corner.

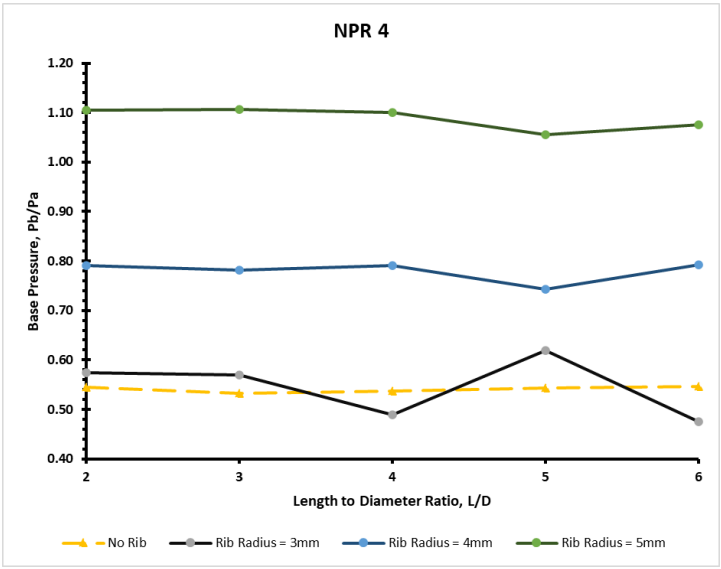

Fig. 8. The base pressure ratio variation with L/D for plain duct and duct with rib at various sizes at NPR 4

For the highest value of NPR = 5, the base pressure results are shown in Figure 9 as a function of the L/D ratio. Due to the increase in the NPR, the level of under-expansion has gone up to 2.7 (i.e., Pe/Pa = 2.7). The figure shows that the base pressure has increased significantly when the rib height is 5 mm, which is forty percent higher than the back pressure. It is also seen that there is a considerable decrease in the base pressure due to the expansion of the nozzle flow at NPR = 5 in the absence of the ribs, and this value has attained as low as 0.4 (P_b/P_a = 0.4). At this level of under-expansion, even ribs with 3 mm result in an increase of the base pressure for all the L/Ds.

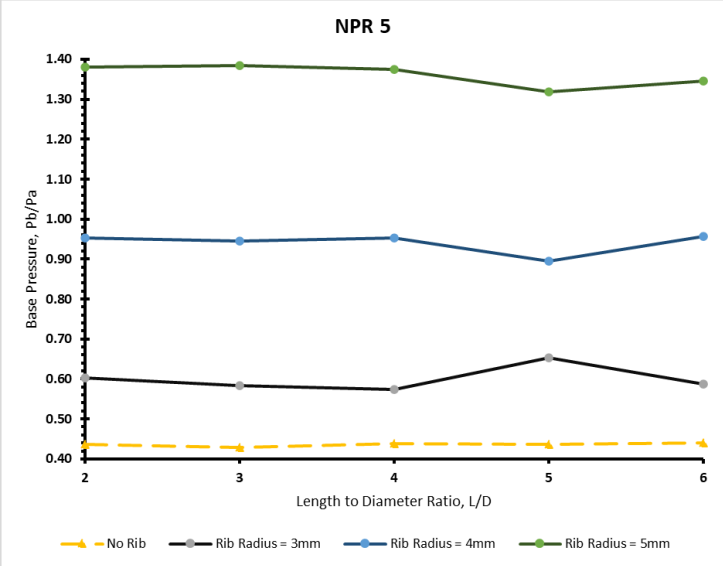

Fig. 9. The base pressure ratio variation with L/D for plain duct and duct with rib at various sizes at NPR 5

3.2 The Influence of Rib and its Geometry Towards Base Pressure with Nozzle Pressure Ratio

Figure 10 shows base pressure results as a function of NPR at L/D = 2 with various rib heights. In the absence of control, there is a continuous decrease in the base pressure. The physics behind this trend maybe when the relief effect due to the increase of the area ratio is beyond some limit, the flow from the nozzle discharged into the enlarged duct tends to attach with a reattachment length other than the optimum for a strong vortex at the base. This process makes the NPR effect on base pressure insignificant for a higher area ratio. When control is employed with rib heights of 3 mm, 4 mm, and 5 mm, with the lowest height of 3 mm, the regulator becomes effective from NPR = 4. These results agree with Rathakrishnan [20] that a rib of height 3 mm decreases the base pressure. He did test for a maximum NPR of 2.58. Hence, he did not experience an increase in the NPR. Therefore, a rib with a height of 3 mm is successful when NPR is four and above. The maximum increase in base pressure is attained for a rib height of 5 mm. Hence, one can select the height of the rib based on the mission requirements. Similar results are seen for L/D = 3 and 4 (Figure 11 to Figure 12); there is a marginal variation in the base pressure values due to increased duct length from 2D to 3D.

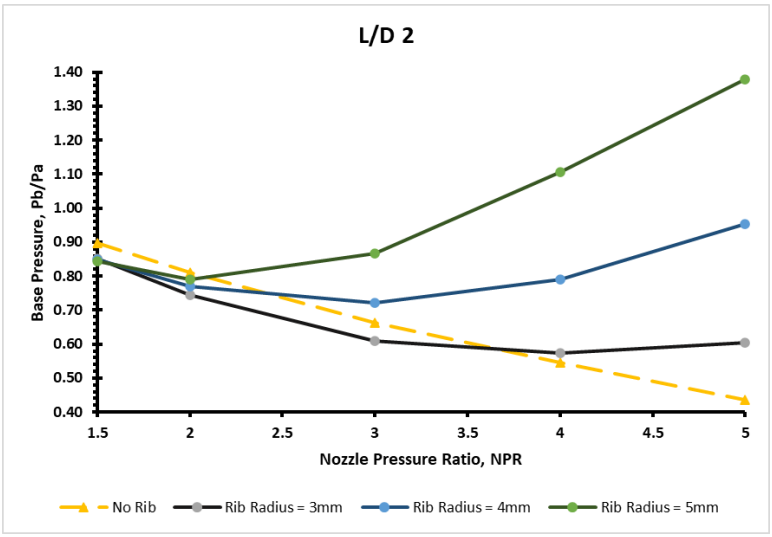

Fig. 10. The base pressure ratio variation with NPR for plain duct and duct with rib at various sizes at L/D 2

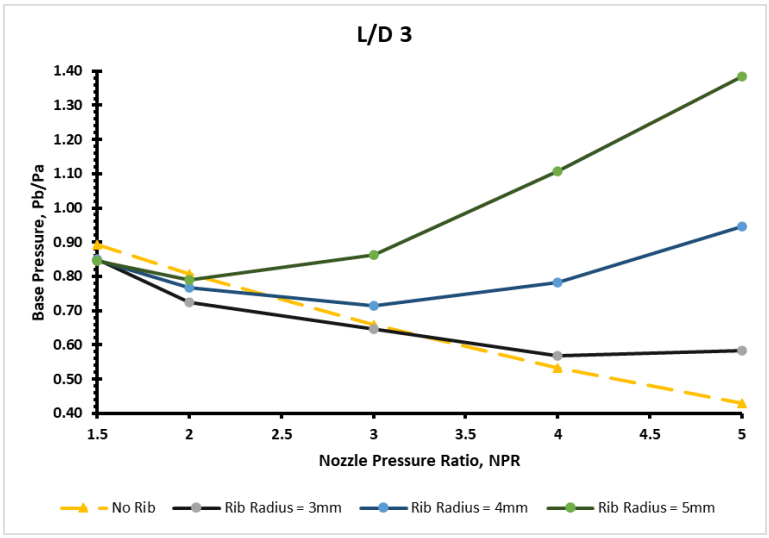

Fig. 11. The base pressure ratio variation with NPR for plain duct and duct with rib at various sizes at L/D 3

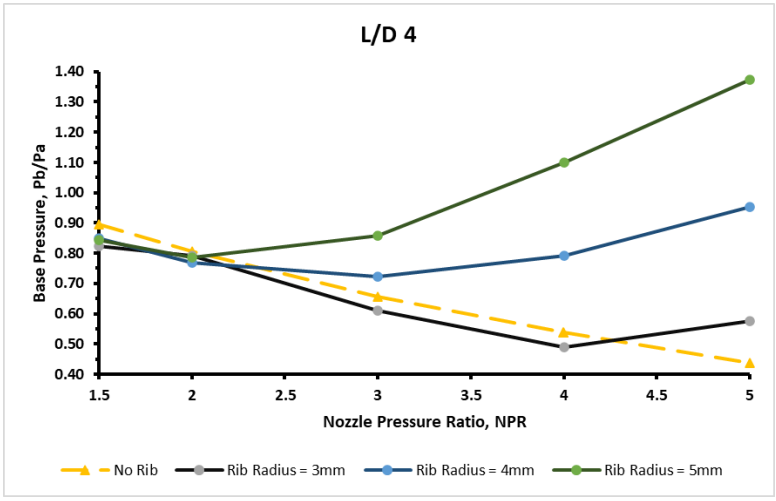

Fig. 12. The base pressure ratio variation with NPR for plain duct and duct with rib at various sizes at L/D 4

The findings of this study for L/D ratio 5 for NPRs in the range from 1.5 to 5 are shown in Figure 13. For this L/D = 5, the base pressure results show a different pattern. When rib height is 3 mm, it becomes influential from NPR = 3 and above, possibly due to the lower influence of atmospheric pressure. Control effectiveness, too, has increased for rib heights of 4 mm and 5 mm. These changes can be attributed to the long duct length, and control in the form of ribs becomes more effective due to the interaction of the shear layer with the secondary vortices.

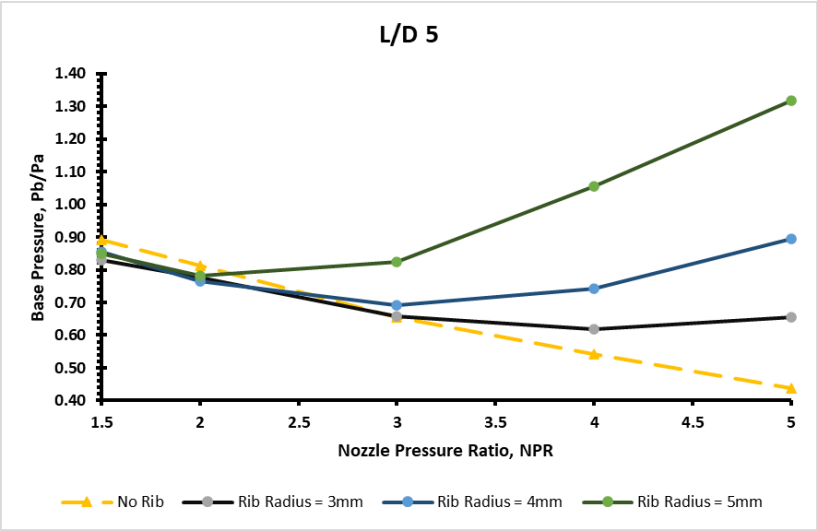

Fig. 13. The base pressure ratio variation with NPR for plain duct and duct with rib at various sizes at L/D 5

As shown in Figure 14, when the L/D increased to 6, the value of the base pressure ratio for the model with a rib size of 3 mm was almost the same as the model without a rib. Then, when the duct length is 6D, the base pressure for the model with rib size 3 mm is the highest from NPR 1.5 to 2 but keeps decreasing until NPR 3, not changing from NPR 3 to 4 and rising back from NPR 4.5 to 5. The trend for models with rib sizes 4mm and 5mm is the same as the other L/D explained earlier. Hence, as we increase the duct length, the base pressure ratio keeps declining even though the nozzle pressure ratio increases. The results for models with rib size 3mm are pretty satisfying for lower duct length. At duct length 2D to 5D, the model with rib size 5mm has the highest base pressure ratio, and it keeps increasing for NPR 2 and above, followed by the model with rib size 4 mm. This change in the base pressure values for rib height of 3 mm is due to the increase in L/D ratio. The flow pattern inside the duct is different due to the interaction between the base vortex, shear layer, and the secondary vortices.

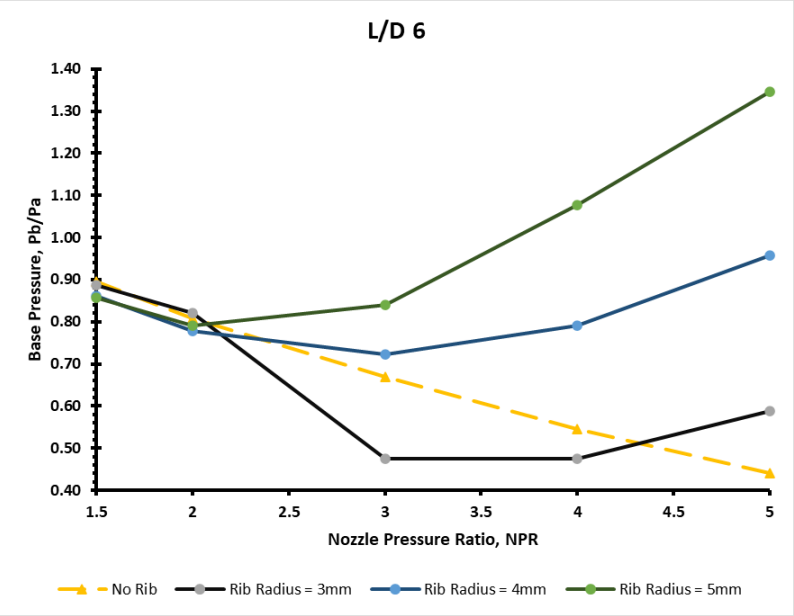

Fig. 14. The base pressure ratio variation with NPR for plain duct and duct with rib at various sizes at L/D 6

3.3 Velocity Contour for Model with Rib Size 5mm

Figure 15 shows the velocity contours for the model suddenly expanded with a duct equipped with a single rib of 5mm in size. The duct length shown above is 2D from the base wall. From Figure 15(a) to Figure 15(e), the value of the nozzle pressure ratio varied from 1.5 to 5.

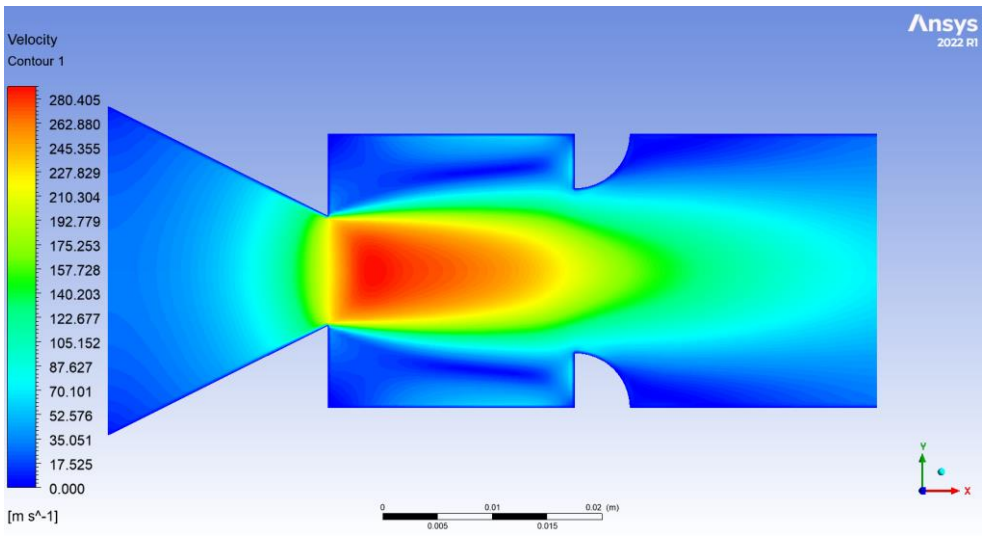

(a) The model suddenly expanded with duct length 2D and NPR 1.5

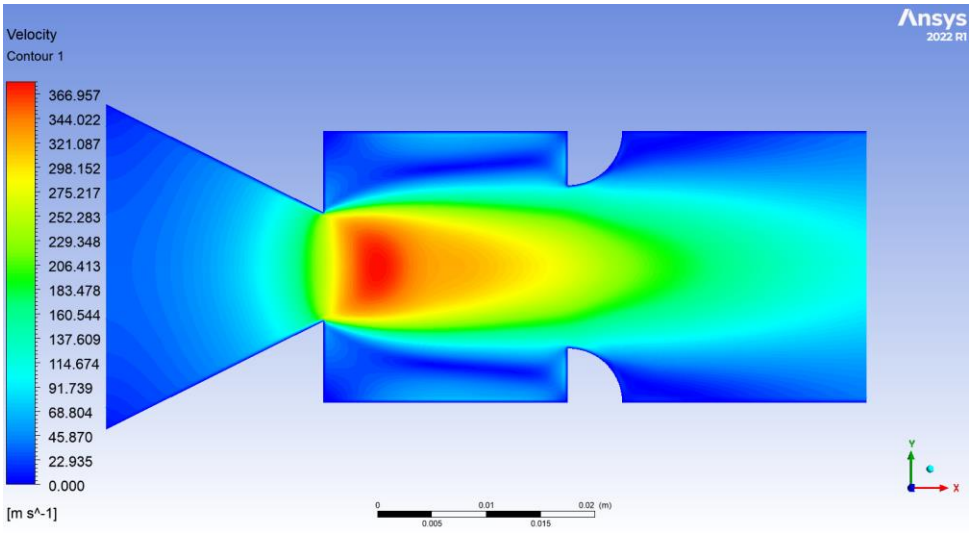

(b) The model suddenly expanded with duct length 2D and NPR 2

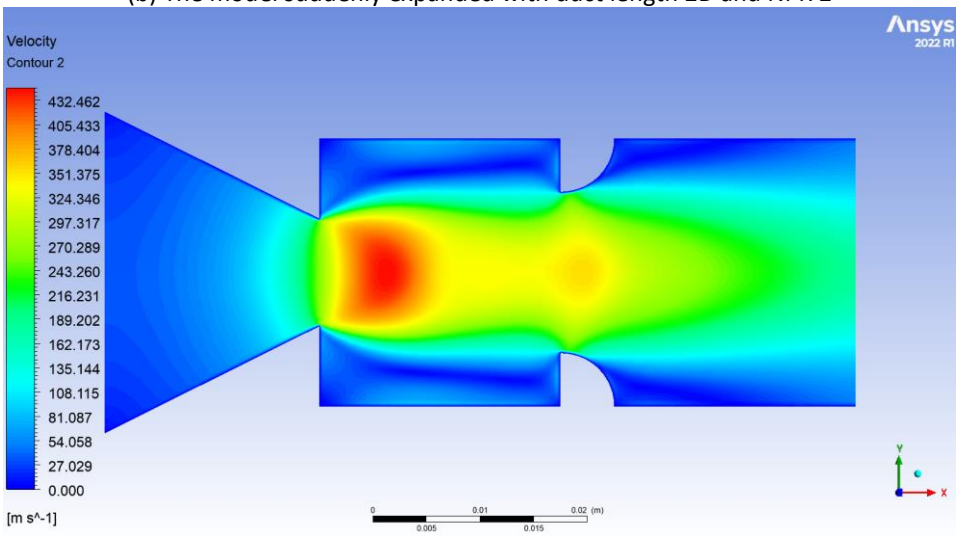

(c) The model suddenly expanded with duct length 2D and NPR 3

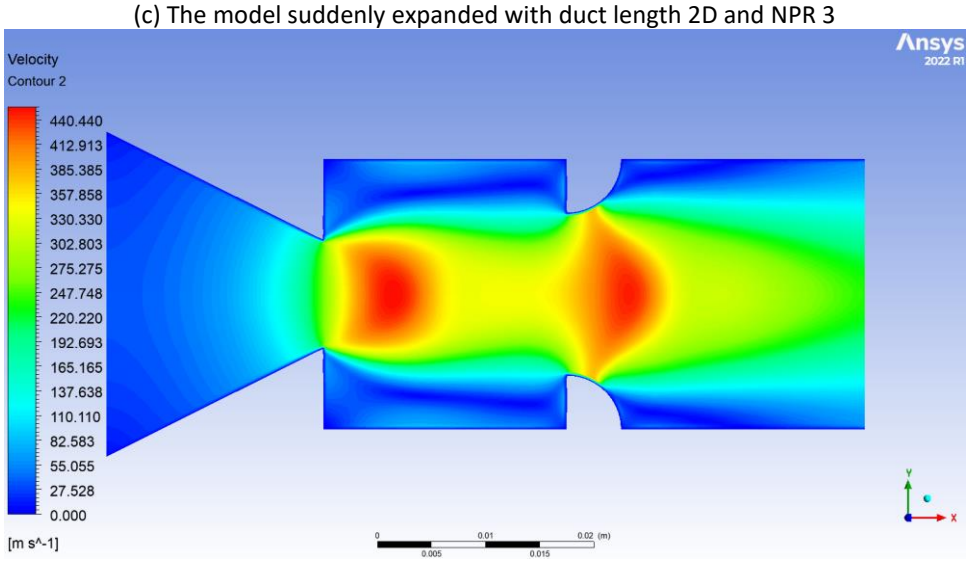

(d) The model suddenly expanded with duct length 2D and NPR 4

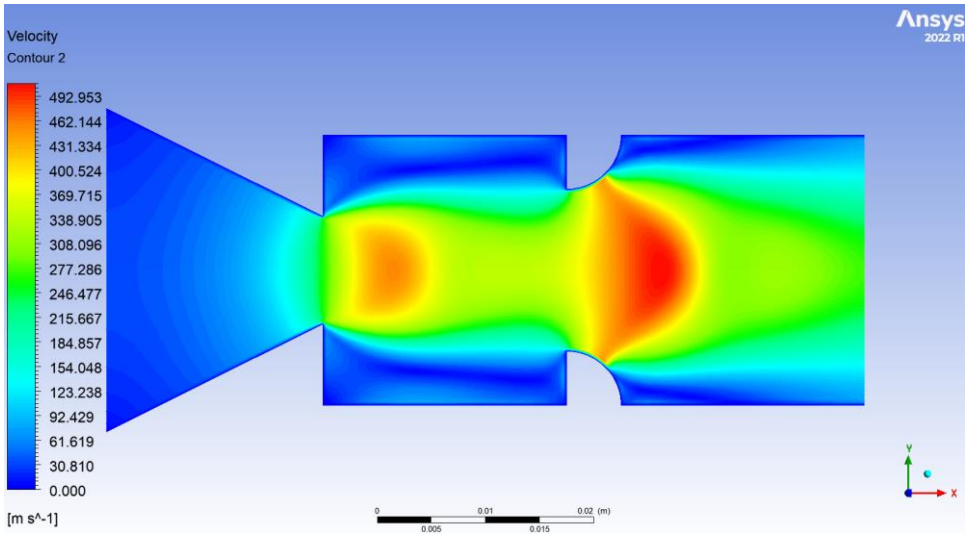

(e) The model suddenly expanded with duct length 2D and NPR 5

Fig. 15. Velocity contours for the model suddenly expanded with a duct equipped with one rib

3.4 Velocity Streamline for Model with Rib Size 5 mm

Figure 16 shows the velocity streamlines for the model suddenly expanded with a duct equipped with a single rib of 5 mm in size. The duct length shown above is 2D from the base wall. From Figure 16(a) to Figure 16(e), the value of the nozzle pressure ratio varied from 1.5 to 5.

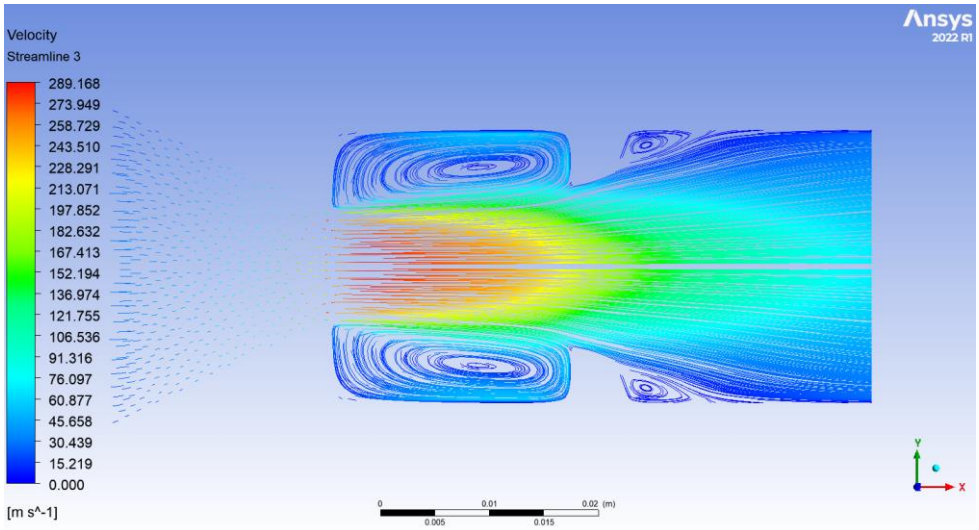

(a) The model suddenly expanded with duct length 2D and NPR 1.5

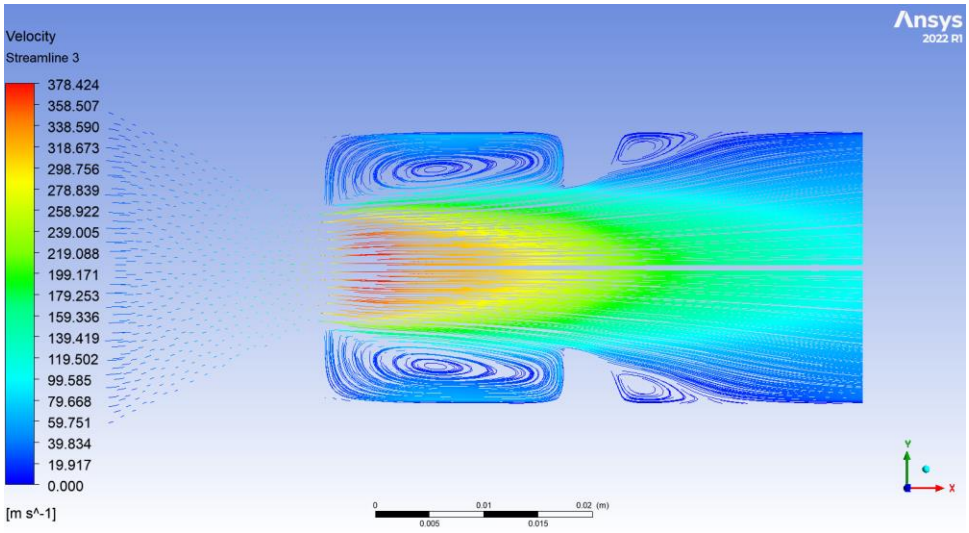

(b) The model suddenly expanded with duct length 2D and NPR 2

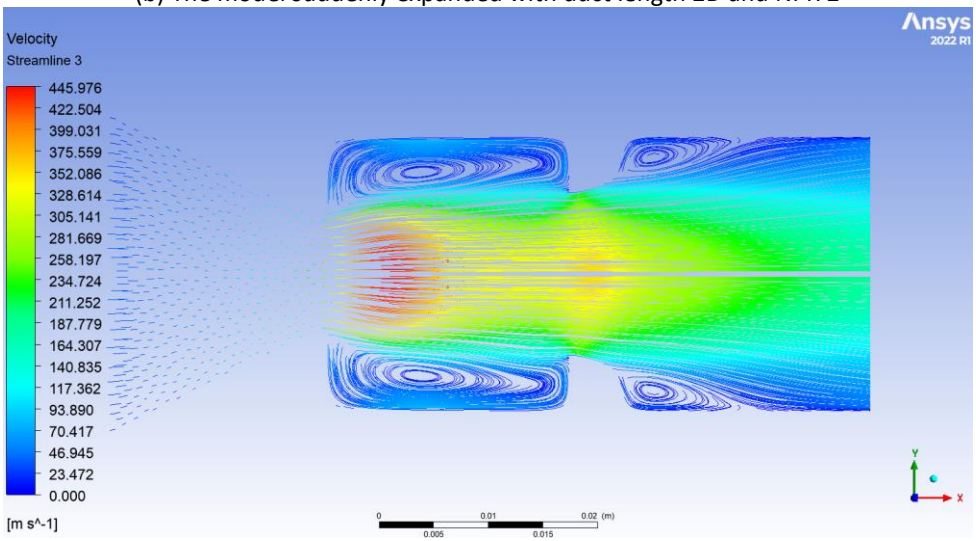

(c) The model suddenly expanded with duct length 2D and NPR 3

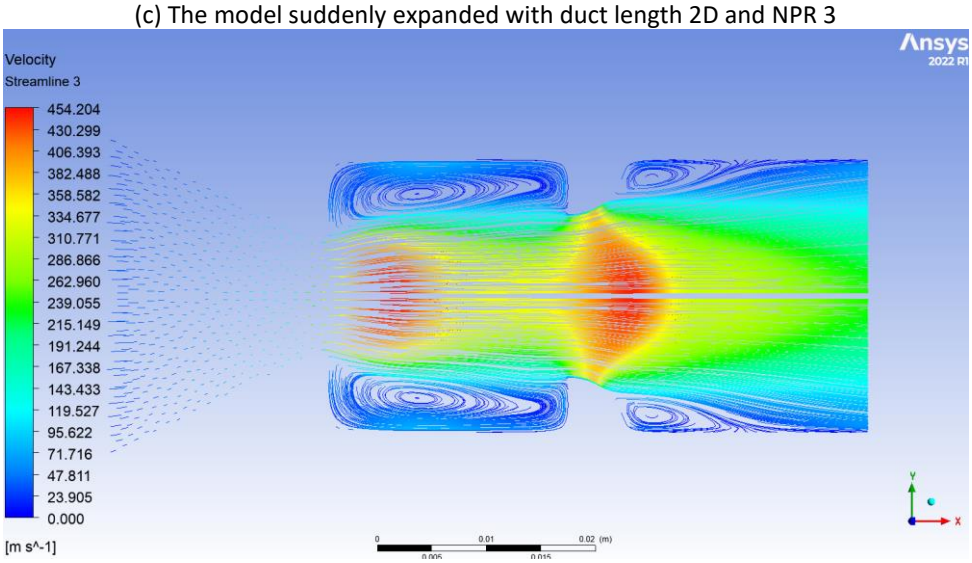

(d) The model suddenly expanded with duct length 2D and NPR 4

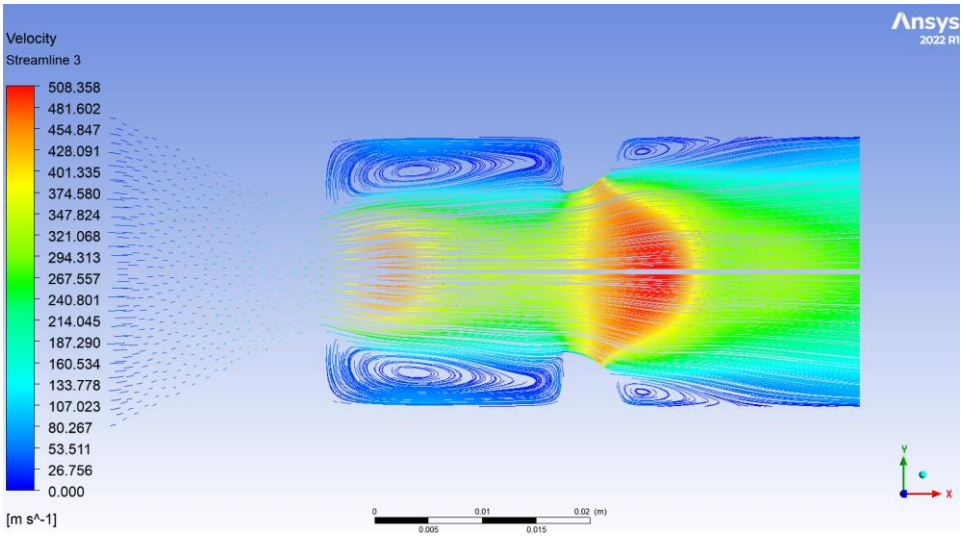

(e) The model suddenly expanded with duct length 2D and NPR 5

Fig. 16. Velocity streamlines for the model suddenly expanded with a duct equipped with one rib

3.5 Pressure Contour for Model with Rib Size 5mm

Figure 17 shows the pressure contours for the model suddenly expanded with a duct equipped with a single rib of 5mm in size. The duct length shown above is 2D from the base wall. From Figure 17(a) to Figure 17(e), the value of the nozzle pressure ratio varied from 1.5 to 5.

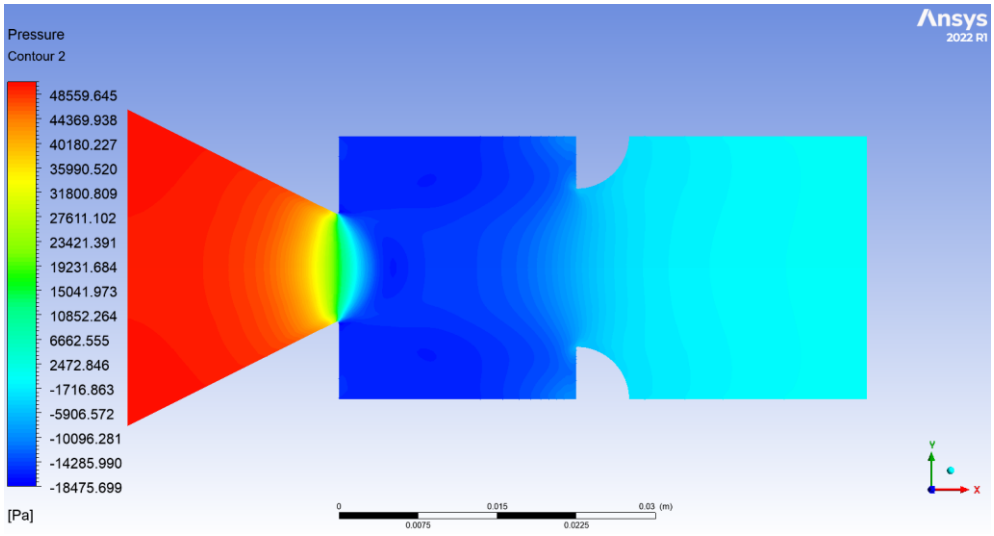

(a) The model suddenly expanded with duct length 2D and NPR 1.5

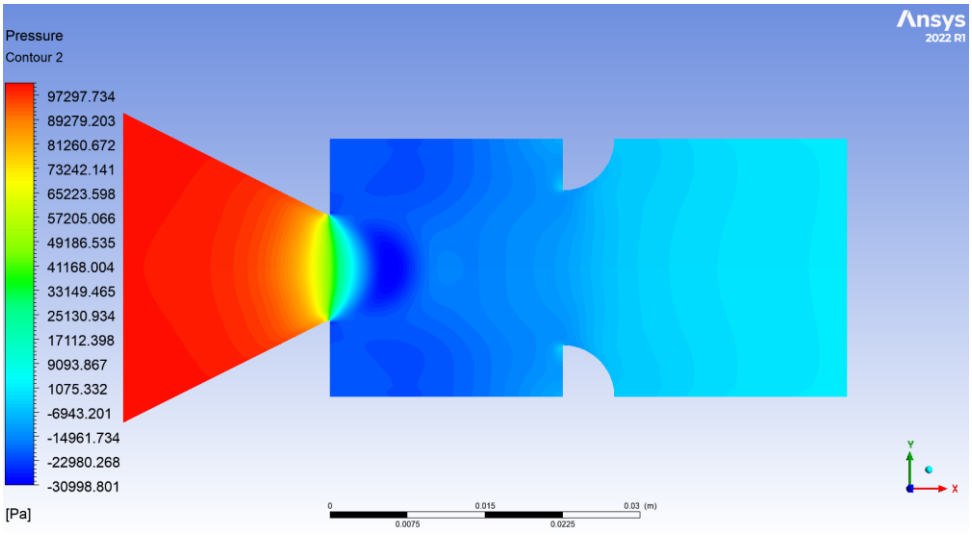

(b) The model suddenly expanded with duct length 2D and NPR 2

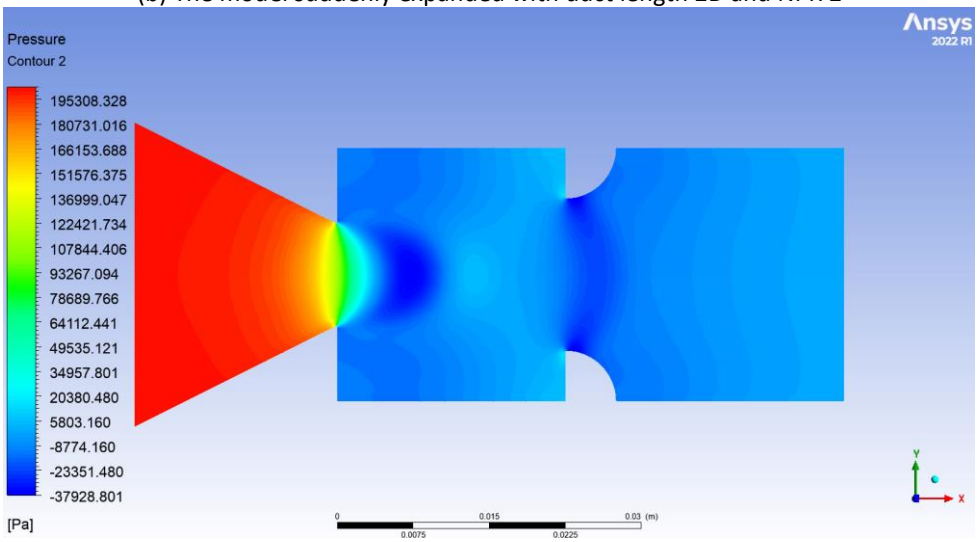

(c) The model suddenly expanded with duct length 2D and NPR 3

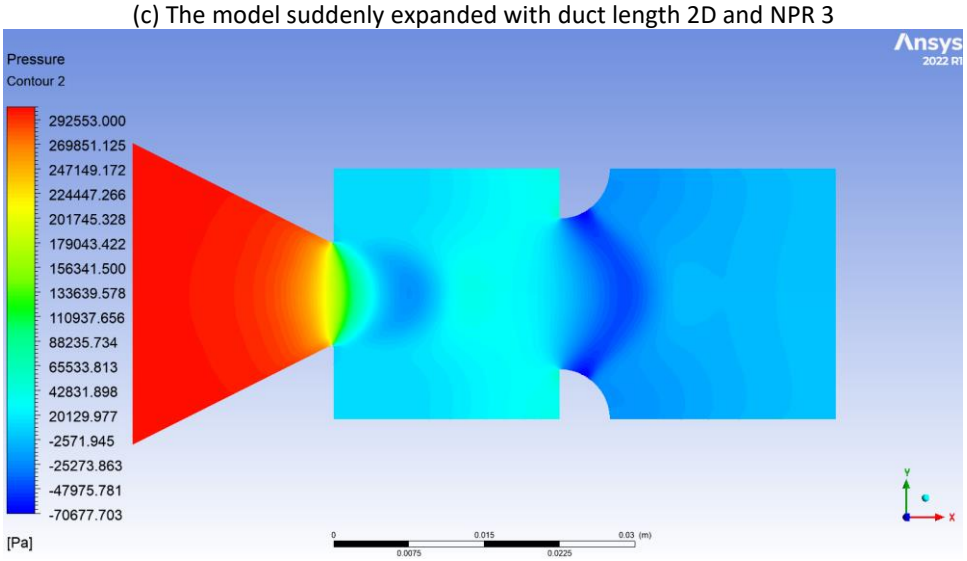

(d) The model suddenly expanded with duct length 2D and NPR 4

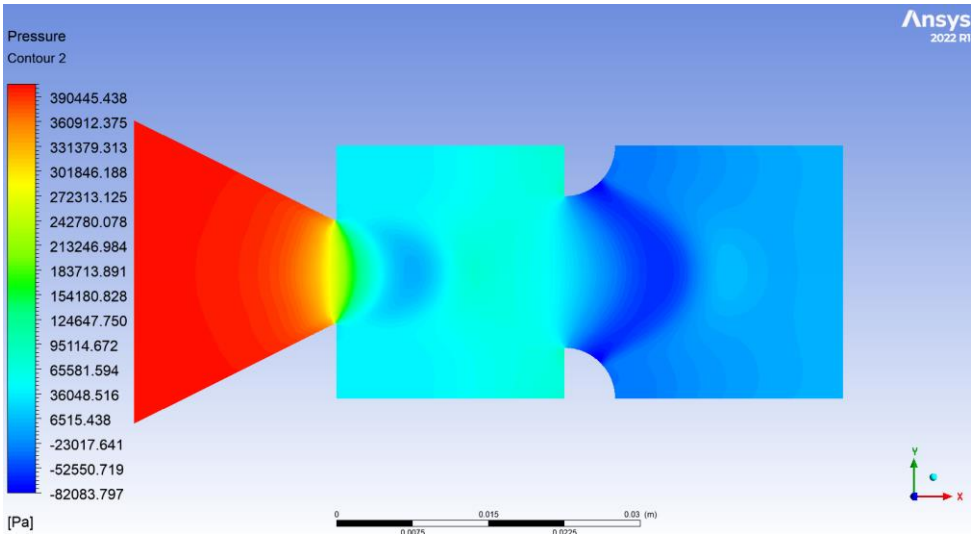

(e) The model suddenly expanded with duct length 2D and NPR 5

Fig. 17. Pressure contours for the model suddenly expanded with a duct equipped with a rib

3.6 Velocity Contour for Model without Rib

Figure 18 shows the velocity contours for the model suddenly expanded with the duct. The duct length shown above is 2D from the base wall. From Figure 18(a) to Figure 18(e), the value of the nozzle pressure ratio varied from 1.5 to 5.

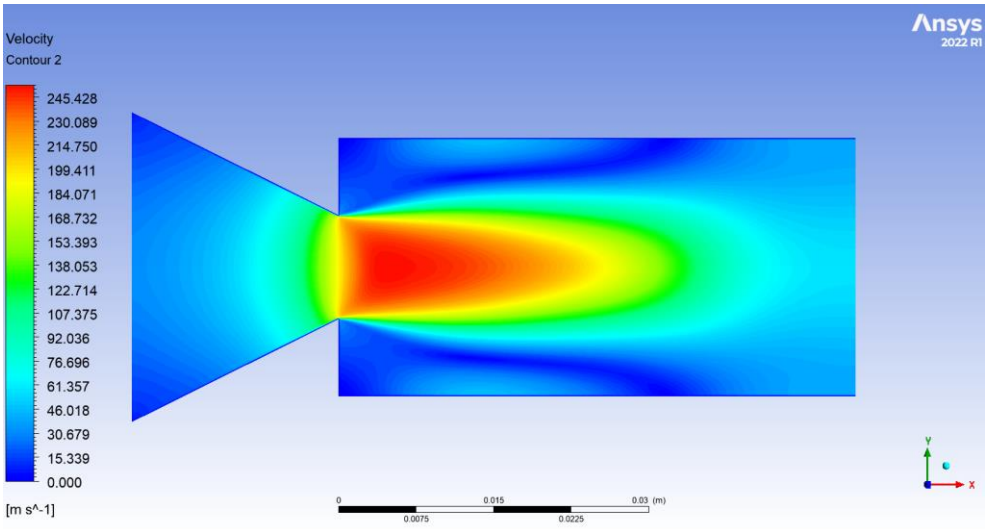

(a) The model suddenly expanded with duct length 2D and NPR 1.5

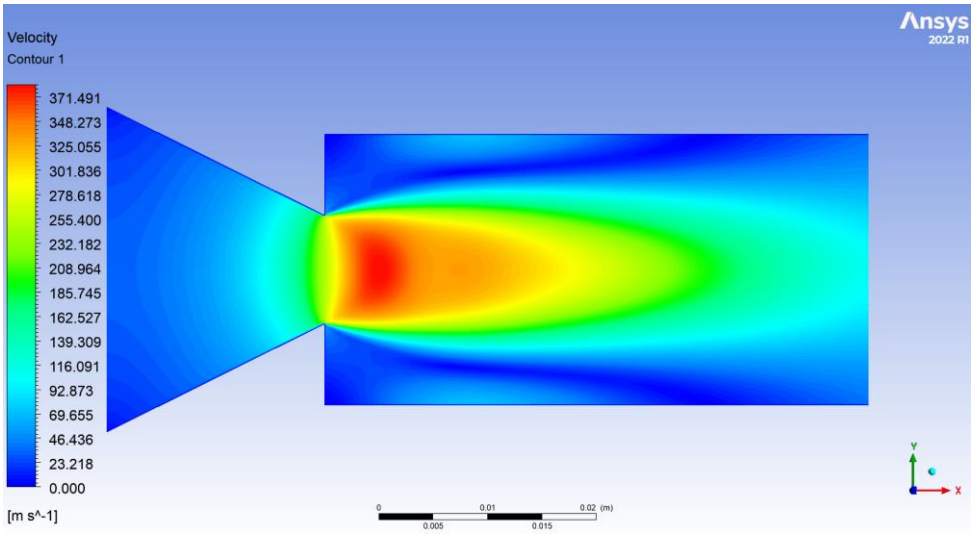

(b) The model suddenly expanded with duct length 2D and NPR 2

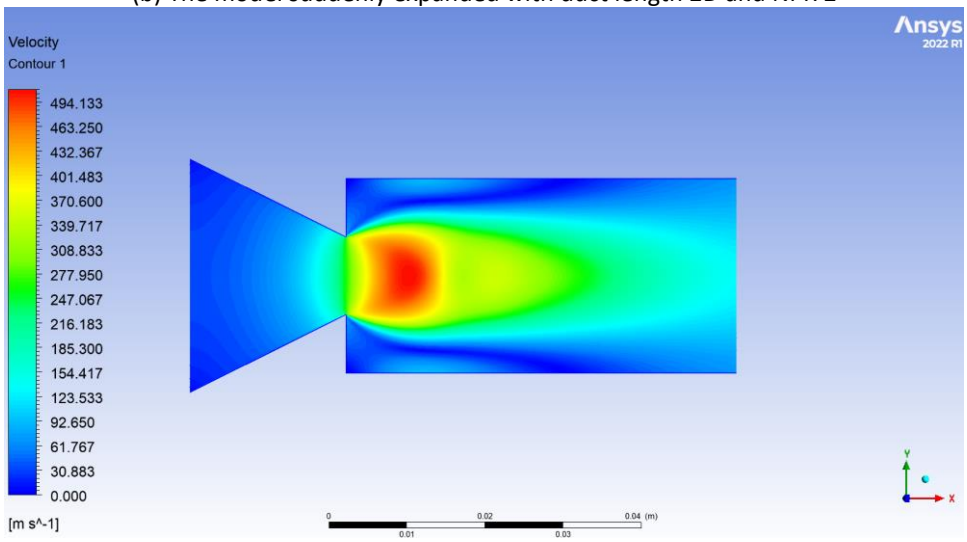

(c) The model suddenly expanded with duct length 2D and NPR 3

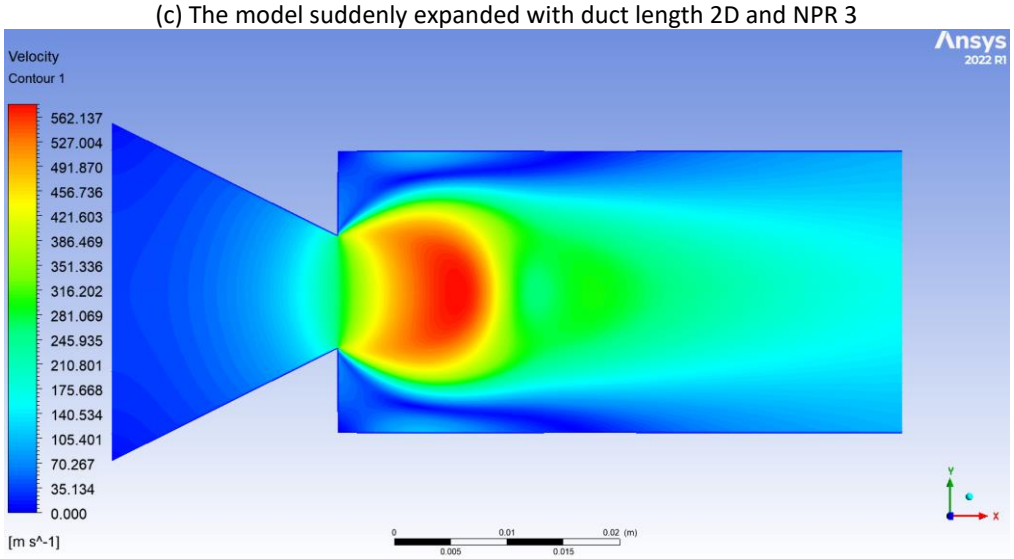

(d) The model suddenly expanded with duct length 2D and NPR 4

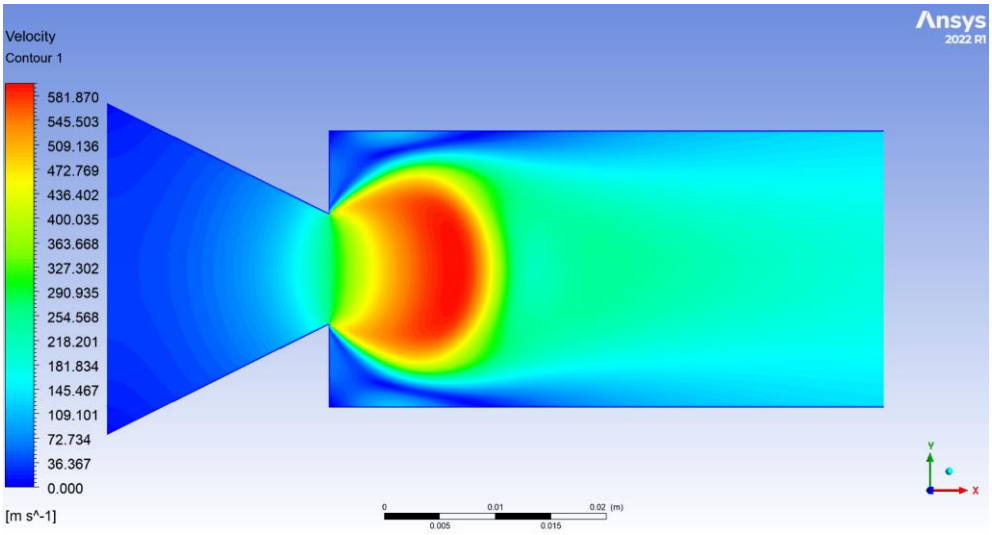

(e) The model suddenly expanded with duct length 2D and NPR 5

Fig. 18. Velocity contours for the model suddenly expanded with duct

3.7 Velocity Streamline for Model without Rib

Figure 19 shows the velocity streamlines for the model suddenly expanded with the duct. The duct length shown above is 2D from the base wall. From Figure 19(a) to Figure 19(e), the value of the nozzle pressure ratio varied from 1.5 to 5.

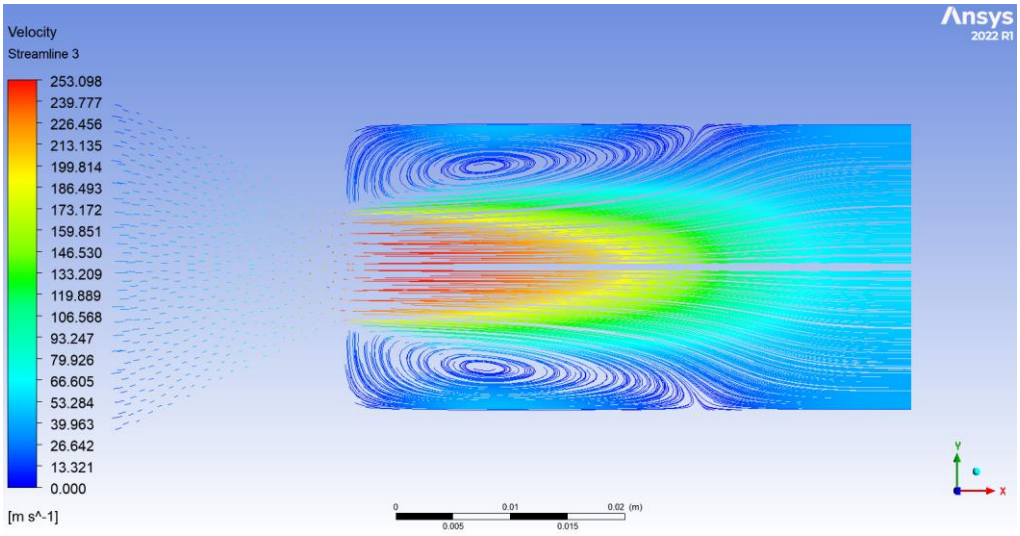

(a) The model suddenly expanded with duct length 2D and NPR 1.5

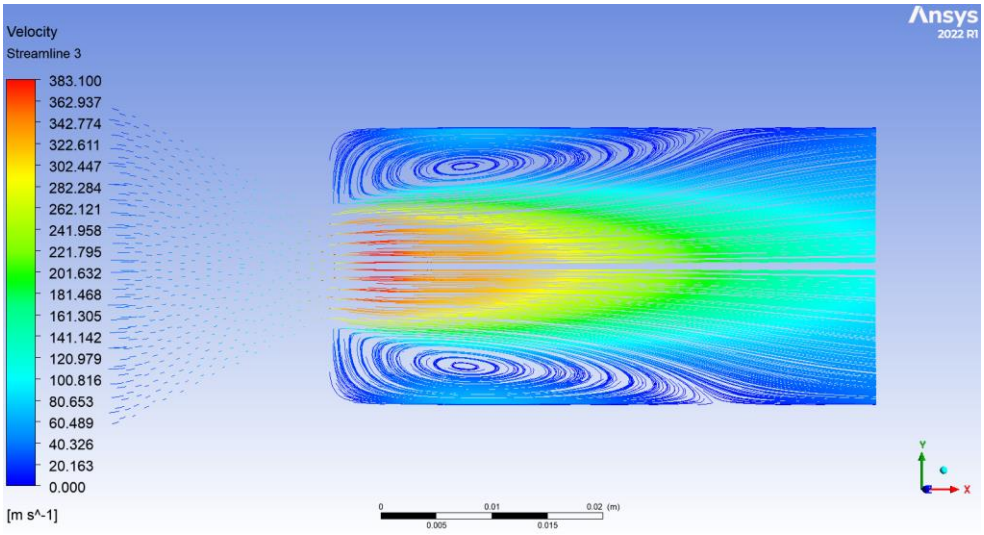

(b) The model suddenly expanded with duct length 2D and NPR 2

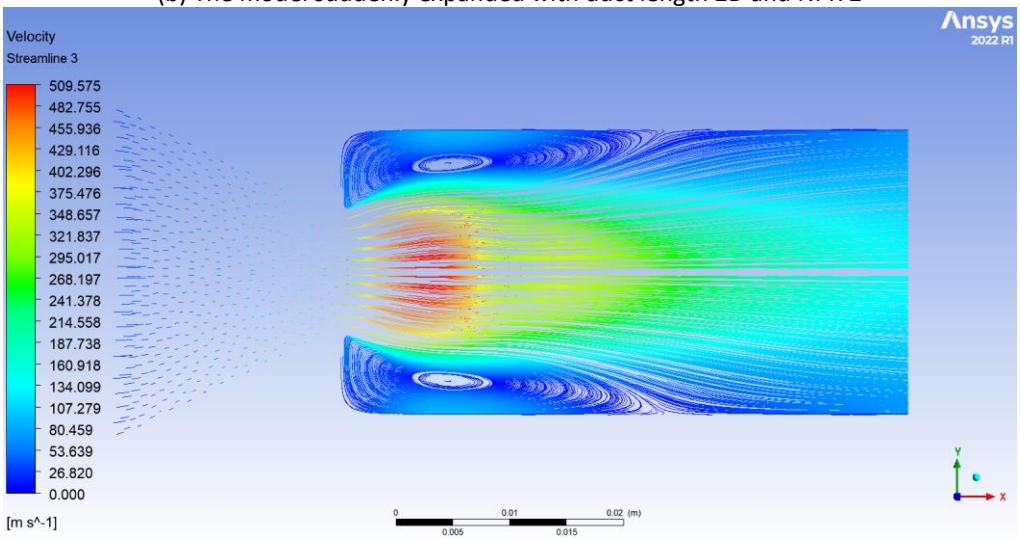

(c) The model suddenly expanded with duct length 2D and NPR 3

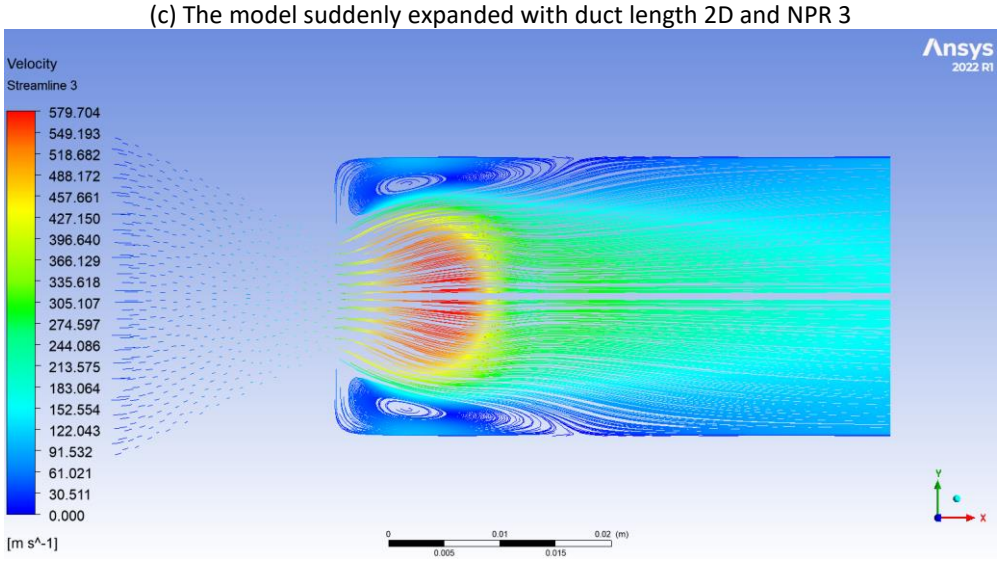

(d) The model suddenly expanded with duct length 2D and NPR 4

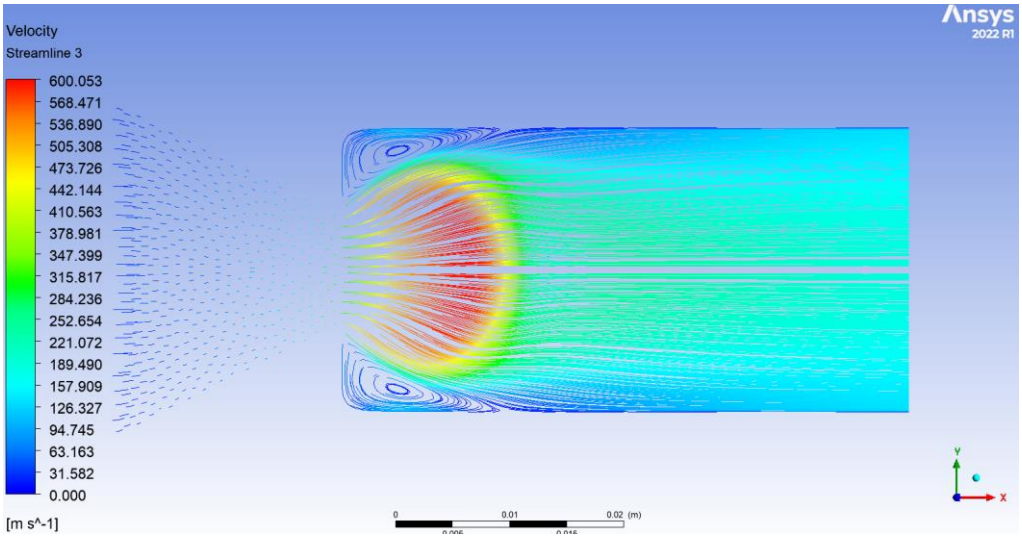

(e) The model suddenly expanded with duct length 2D and NPR 5

Fig. 19. Velocity streamline for model suddenly expanded with duct

3.8 Pressure Contour for Model without Rib

Figure 20 shows the pressure contours for the model suddenly expanded with the duct. The duct length shown above is 2D from the base wall. From Figure 20(a) to Figure 20(e), the value of the nozzle pressure ratio varied from 1.5 to 5.

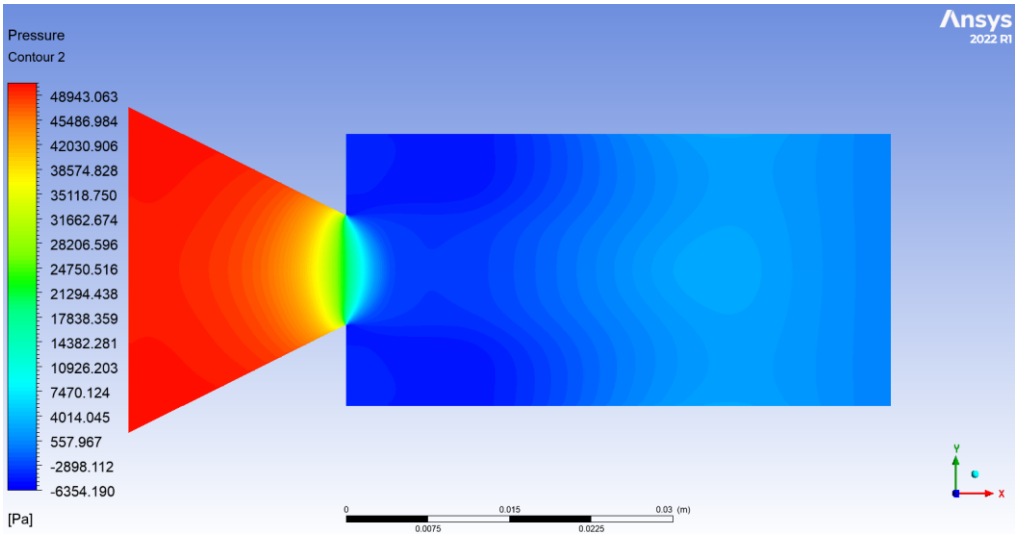

(a) The model suddenly expanded with duct length 2D and NPR 1.5

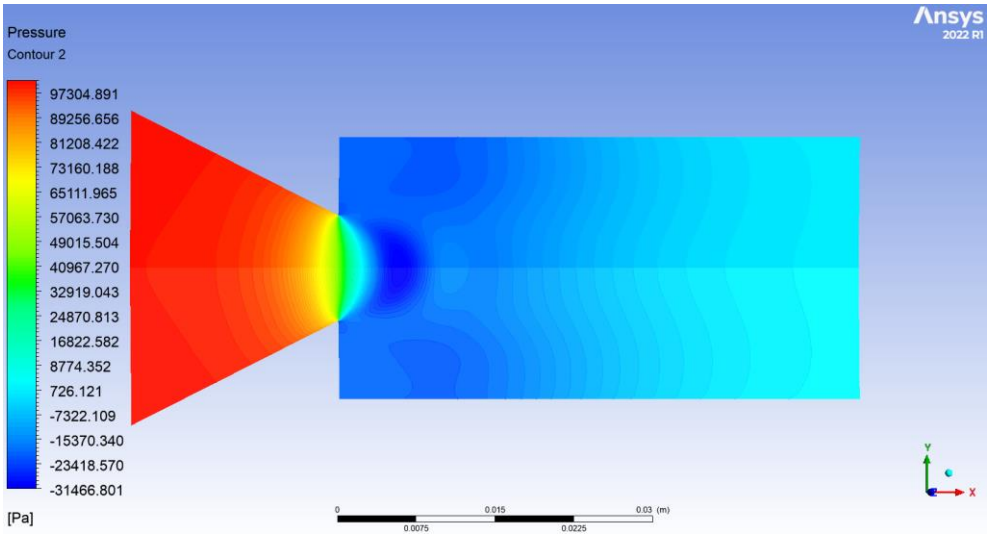

(b) The model suddenly expanded with duct length 2D and NPR 2

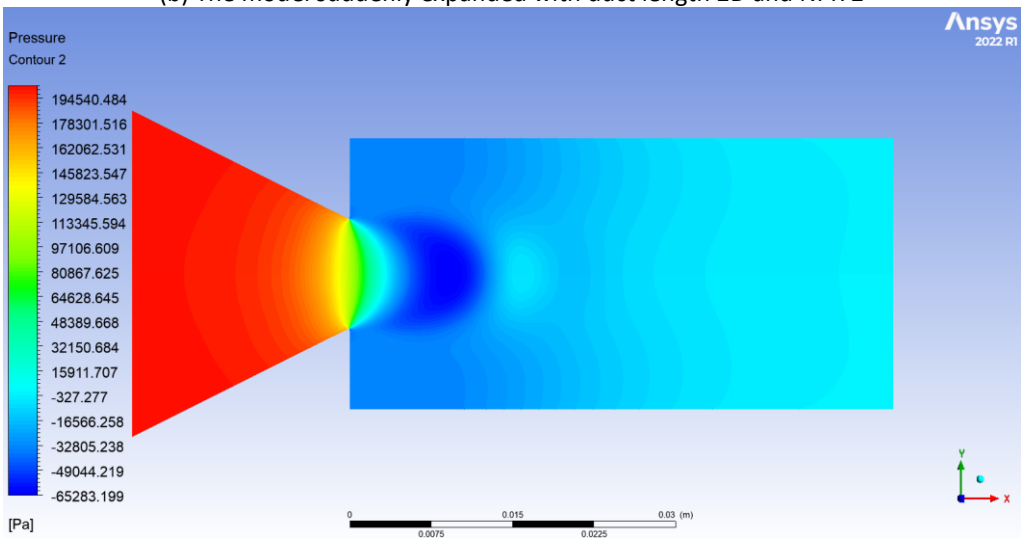

(c) The model suddenly expanded with duct length 2D and NPR 3

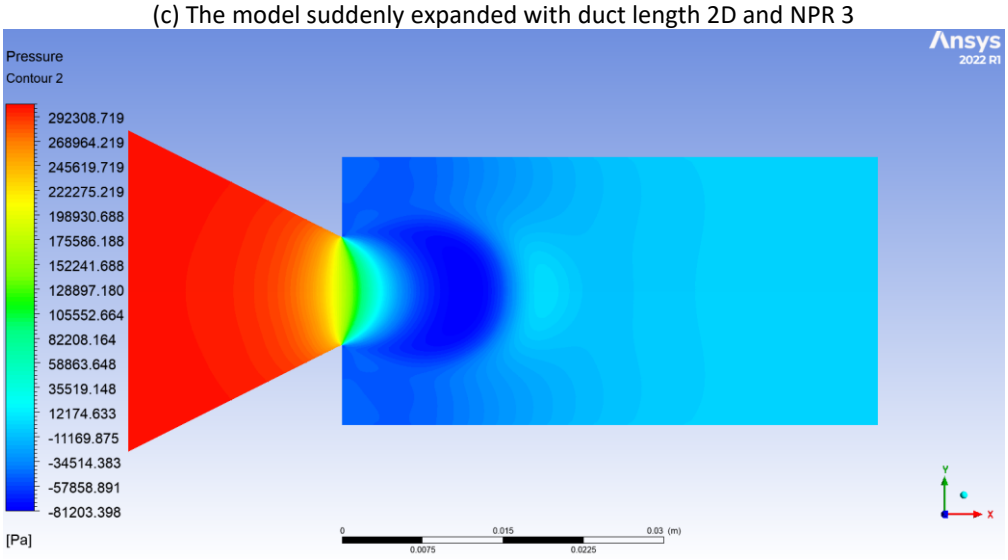

(d) The model suddenly expanded with duct length 2D and NPR 4

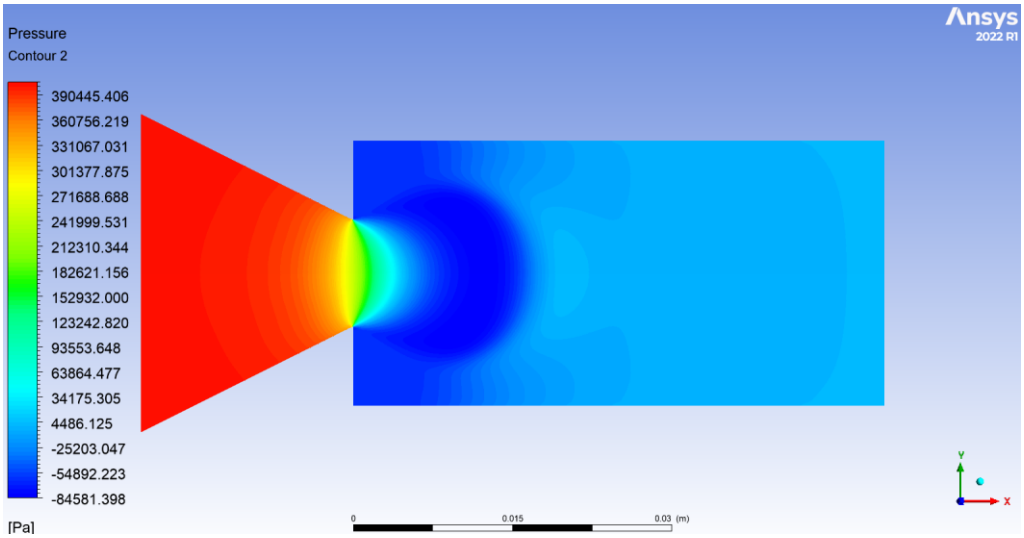

(e) The model suddenly expanded with duct length 2D and NPR 5

Fig. 20. Pressure contours for the model suddenly expanded with duct

4. Conclusion

Based on the above discussion, we may conclude that the base pressure for a model with plain duct keeps decreasing as the NPR increases and the area ratio 6.25 is high. The base pressure for the model with rib diameter keeps rising as the NPR increases. The L/D ratio plays a vital role in fixing the base pressure values. At higher NPR, it can be stated that the bigger the rib size, the higher the base pressure. The base pressure value did not solely depend on NPR. It also depended on other characteristics, such as rib size and L/D ratio. At NPR 4 and 5, the base pressure for the model with a rib diameter of 5 mm is more than the ambient pressure due to the duct having smaller space for the flow to expand. The base pressure also changes to some extent as we increase the L/D ratio, except for the model with a rib diameter of 3 mm, which is unstable when the L/D increases. The pressure gradient based on contour results demonstrates that the passive control in the form of ribs does not adversely affect the wall pressure. Ribs with a height of 3 mm become effective for four and above, whereas those with a height of 4 mm and 5 mm are effective once the nozzle has reached critical condition. For example, rib size and orientation are significant in manipulating the result. However, the rib does not adversely impact the flow in the duct. The users can choose the height of the ribs based on the mission requirements. If the mission requires increasing the base pressure, then ribs of 4 mm and 5 mm are the right choice.

References

[1] Nusselt, W. "Heat dissipation from horizontal tubes and wires to gases and liquids." *Ver Deutlng* 73 (1929): 1475-1478.

[2] Wick, Robert S. "The effect of boundary layer on sonic flow through an abrupt cross-sectional area change." *Journal of the Aeronautical Sciences* 20, no. 10 (1953): 675-682. https://doi.org/10.2514/8.2794

[3] Pandey, K. M., and E. Rathakrishnan. "Annular cavities for Base flow control." *International Journal of Turbo and Jet Engines* 23, no. 2 (2006): 113-128. https://doi.org/10.1515/TJJ.2006.23.2.113

[4] Pesce, Vincenzo, Stefano Silvestrini, and Michèle Lavagna. "Radial basis function neural network aided adaptive extended Kalman filter for spacecraft relative navigation." *Aerospace Science and Technology* 96 (2020): 105527. https://doi.org/10.1016/j.ast.2019.105527

[5] Al-Daraje, H. Yousif, and Nabeh N. Alderoubi. "Effect of combination yaw angle variation and base bleeding for tractor-trailer drag reduction through experimental investigation and CFD." In *Journal of Physics: Conference Series*, vol. 1519, no. 1, p. 012017. IOP Publishing, 2020. https://doi.org/10.1088/1742-6596/1519/1/012017

[6] Zhou, Jian-xun, Cheng-hong Sun, and Daichin Daichin. "Drag reduction and flow structures of wing tip sails in ground

effect." *Journal of Hydrodynamics* 32, no. 1 (2020): 93-106. https://doi.org/10.1007/s42241-020-0006-4
[7] Gao, Shiqi, and Jinkun Liu. "Adaptive neural network vibration control of a flexible aircraft wing system with input signal quantization." *Aerospace Science and Technology* 96 (2020): 105593. https://doi.org/10.1016/j.ast.2019.105593
[8] Li, Shibin, Langquan Li, Wei Huang, Yilong Zhao, and Jian Chen. "Design and investigation of equal cone-variable Mach number waverider in hypersonic flow." *Aerospace Science and Technology* 96 (2020): 105540. https://doi.org/10.1016/j.ast.2019.105540
[9] Lu, Junjie, Jinquan Huang, and Feng Lu. "Kernel extreme learning machine with iterative picking scheme for failure diagnosis of a turbofan engine." *Aerospace Science and Technology* 96 (2020): 105539. https://doi.org/10.1016/j.ast.2019.105539
[10] Yan, Cheng, Zeyong Yin, Xiuli Shen, Dong Mi, Fushui Guo, and Dan Long. "Surrogate-based optimization with improved support vector regression for non-circular vent hole on aero-engine turbine disk." *Aerospace Science and Technology* 96 (2020): 105332. https://doi.org/10.1016/j.ast.2019.105332
[11] Rathakrishnan, E., O. V. Ramanaraju, and K. Padmanaban. "Influence of cavities on suddenly expanded flow field." *Mechanics Research Communications* 16, no. 3 (1989): 139-146. https://doi.org/10.1016/0093-6413(89)90051-7
[12] Pandey, Krishna Murari, and E. Rathakrishnan. "Influence of cavities on flow development in sudden expansion." *International Journal of Turbo and Jet Engines* 23, no. 2 (2006): 97-112. https://doi.org/10.1515/TJJ.2006.23.2.97
[13] Pathan, Khizar Ahmed, Prakash S. Dabeer, and Sher Afghan Khan. "Effect of nozzle pressure ratio and control jets location to control base pressure in suddenly expanded flows." *Journal of Applied Fluid Mechanics* 12, no. 4 (2019): 1127-1135. https://doi.org/10.29252/jafm.12.04.29495
[14] Vikramaditya, N. S., M. Viji, S. B. Verma, Naveed Ali, and D. N. Thakur. "Base pressure fluctuations on typical missile configuration in presence of base cavity." *Journal of Spacecraft and Rockets* 55, no. 2 (2018): 335-345. https://doi.org/10.2514/1.A33926
[15] Khan, Sher Afghan, Mohammed Asadullah, GM Fharukh Ahmed, Ahmed Jalaluddeen, and Maughal Ahmed Ali Baig. "Passive control of base drag in compressible subsonic flow using multiple cavity." *International Journal of Mechanical and Production Engineering Research and Development (IJMPERD)* 8, no. 4 (2018): 39-44. https://doi.org/10.24247/ijmperdaug20185
[16] Asadullah, Mohammed, Sher Afghan Khan, Manzoore Elahi M. Soudagar, and T. R. Vaishak. "A comparison of the effect of single and multiple cavities on base flows." In *2018 IEEE 5th International Conference on Engineering Technologies and Applied Sciences (ICETAS)*, pp. 1-6. IEEE, 2018. https://doi.org/10.1109/ICETAS.2018.8629196
[17] Sethuraman, Vigneshvaran, Parvathy Rajendran, and Sher Afghan Khan. "A Cost-effective Data Acquisition Instrumentation for Measurement of Base Pressure and Wall Pressure in Suddenly Expanded Flow Through Ducts." *Journal of Advanced Research in Fluid Mechanics and Thermal Sciences* 60, no. 1 (2019): 112-123.
[18] Afzal, Asif, Abdul Aabid, Ambareen Khan, Sher Afghan Khan, Upendra Rajak, Tikendra Nath Verma, and Rahul Kumar. "Response surface analysis, clustering, and random forest regression of pressure in suddenly expanded high-speed aerodynamic flows." *Aerospace Science and Technology* 107 (2020): 106318. https://doi.org/10.1016/j.ast.2020.106318
[19] Afzal, Asif, Sher Afghan Khan, Md Tariqul Islam, R. D. Jilte, Ambareen Khan, and Manzoore Elahi M. Soudagar. "Investigation and back-propagation modeling of base pressure at sonic and supersonic Mach numbers." *Physics of Fluids* 32, no. 9 (2020): 096109. https://doi.org/10.1063/5.0022015
[20] Rathakrishnan, E. "Effect of ribs on suddenly expanded flows." *AIAA Journal* 39, no. 7 (2001): 1402-1404. https://doi.org/10.2514/2.1461
[21] Vijayaraja, K. "Effect of rib on suddenly expanded supersonic flow." *Faculty of Mechanical Engineering, Anna University*, 2008.
[22] Vijayaraja, K., C. Senthilkumar, S. Elangovan, and E. Rathakrishnan. "Base pressure control with annular ribs." *International Journal of Turbo & Jet-Engines* 31, no. 2 (2014): 111-118. https://doi.org/10.1515/tjj-2013-0037
[23] Ridwan, Ridwan, Nur Husnina Muhamad Zuraidi, Istiyak Mudassir Shaik, and Sher Afghan Khan. "Passive Control of Base Pressure Using Cavities in A Sudden Expansion Duct: A CFD Approach." *Journal of Mechanical Engineering Research and Developments* 45, no. 3 (2022): 44-70.
[24] Ridwan, Ridwan, Nur Husnina Muhamad Zuraidi, and Sher Afghan Khan. "Impact of Cavity Location on Base Pressure at Supersonic Mach 1.8." *Journal of Mechanical Engineering Research and Developments* 45, no. 2 (2022): 123-150.
[25] Zuraidi, Nur Husnina Muhamad, Sher Afghan Khan, Abdul Aabid, Muneer Baig, and Istiyaq Mudassir Shaiq. "Passive control of base pressure in a converging-diverging nozzle with area ratio 2.56 at Mach 1.8." *Fluid Dynamics & Materials Processing* 19 (2023): 807-829. https://doi.org/10.32604/fdmp.2023.023246
[26] Baig, M. Ahmed Ali, Sher Afghan Khan, and E. Rathakrishnan. "Active control of base pressure in suddenly expanded flow for area ratio 4.84." *International Journal of Engineering Science and Technology* 4, no. 5 (2012): 1892-1902.

[27] Fharukh, Ahmed G. M., and Sher Afghan Khan. "Active control of base pressure using micro jets for area ratio of 7.56." *International Journal of Innovative Technology and Exploring Engineering (IJITEE)* 8, no. 6S3 (2019): 491-495.
[28] Asad Ullah, Mohammed, Musavir Bashir, Ayub Janvekar, and S. A. Khan. "Active control of wall pressure flow field at low supersonic Mach numbers." *IOSR Journal of Mechanical and Civil Engineering* 16, no. 053 (2016): 90-98. https://doi.org/10.9790/1684-16053039098
[29] Ashfaq, Syed, Sher Afghan Khan, and E. Rathakrishnan. "Active Control of Flow through the Nozzles at Sonic Mach Number." *International Journal of Emerging Trends in Engineering and Development* 2, no. 3 (2013): 73-82.
[30] Azami, Muhammed Hanafi, Mohammed Faheem, Abdul Aabid, Imran Mokashi, and Sher Afghan Khan. "Inspection of supersonic flows in a CD nozzle using experimental method." *International Journal of Recent Technology and Engineering* 8, no. 2S3 (2019): 996-999. https://doi.org/10.35940/ijrte.B1186.0782S319
[31] Khan, Sher Afghan, Abdul Aabid, and Ahamed Saleel Chandu Veetil. "Influence of micro jets on the flow development in the enlarged duct at supersonic Mach number." *International Journal of Mechanical and Mechatronics Engineering* 19, no. 1 (2019): 70-82.
[32] Fharukh, Ahmed GM, Mohammad Asad Ullah, and Sher Afghan Khan. "Experimental study of suddenly expanded flow from correctly expanded nozzles." *ARPN Journal of Engineering and Applied Sciences* 11, no. 16 (2016): 10041-10047.
[33] Pathan, Khizar A., Prakash S. Dabeer, and Sher A. Khan. "Enlarge duct length optimization for suddenly expanded flows." *Advances in Aircraft and Spacecraft Science* 7, no. 3 (2020): 203-214.
[34] Pathan, Khizar Ahmed, Prakash S. Dabeer, and Sher Afghan Khan. "Influence of expansion level on base pressure and reattachment length." *CFD Letters* 11, no. 5 (2019): 22-36.
[35] Khan, Sher Afghan, Abdul Aabid, Fharukh Ahmed Mehaboobali Ghasi, Abdulrahman Abdullah Al-Robaian, and Ali Sulaiman Alsagri. "Analysis of area ratio in a CD nozzle with suddenly expanded duct using CFD method." *CFD Letters* 11, no. 5 (2019): 61-71.
[36] Aabid, Abdul, and Sher Afghan Khan. "Investigation of high-speed flow control from CD nozzle using design of experiments and CFD methods." *Arabian Journal for Science and Engineering* 46, no. 3 (2021): 2201-2230. https://doi.org/10.1007/s13369-020-05042-z
[37] Sajali, Muhammad Fahmi Mohd, Abdul Aabid, Sher Afghan Khan, Fharukh Ahmed Ghasi Mehaboobali, and Erwin Sulaeman. "Numerical Investigation of Flow Field of a Non-Circular Cylinder." *CFD Letters* 11, no. 5 (2019): 37-49.
[38] Khan, Sher Afghan, Abdul Aabid, and C. Ahamed Saleel. "CFD simulation with analytical and theoretical validation of different flow parameters for the wedge at supersonic Mach number." *International Journal of Mechanical and Mechatronics Engineering* 19, no. 1 (2019): 170-177.
[39] Khan, Ambareen, Parvathy Rajendran, Junior Sarjit Singh Sidhu, S. Thanigaiarasu, Vijayanandh Raja, and Qasem Al-Mdallal. "Convolutional neural network modeling and response surface analysis of compressible flow at sonic and supersonic Mach numbers." *Alexandria Engineering Journal* 65 (2023): 997-1029. https://doi.org/10.1016/j.aej.2022.10.006
[40] Khan, Ambareen, Parvathy Rajendran, and Junior Sarjit Singh Sidhu. "Passive control of base pressure: a review." *Applied Sciences* 11, no. 3 (2021): 1334. https://doi.org/10.3390/app11031334
[41] Khan, Ambareen, Nurul Musfirah Mazlan, and Ervin Sulaeman. "Effect of Ribs as Passive Control on Base Pressure at Sonic Mach Numbers." *CFD Letters* 14, no. 1 (2022): 140-151. https://doi.org/10.37934/cfdl.14.1.140151
[42] Khan, Ambareen, Mohd Azmi Ismail, and Nurul Musfirah Mazlan. "Numerical Simulation of Suddenly Expanded Flow from Converging Nozzle at Sonic Mach Number." In *Proceedings of International Conference of Aerospace and Mechanical Engineering 2019: AeroMech 2019*, 20-21 November 2019, Universiti Sains Malaysia, Malaysia, pp. 349-359. Springer Singapore, 2020. https://doi.org/10.1007/978-981-15-4756-0_29
[43] Cengel, Yunus A., and John Cimbala. *Fluid mechanics: fundamentals and applications*. McGraw-Hill, 2017.